CHAPTER 1
INTRODUCTION

The manufacturing process of sheet metal forming is one of the very important processing technologies in the modern manufacturing industry used in mass production, to produce automobile components of different configurations. Among the sheet metal forming operations, deep drawing process accounts for a larger proportion. In addition to the sustenance of the required strength and rigidity, the manufactured products can enjoy the advantages of lightweight and suitability for mass production, making the application scope of metal forming become more extensive. In order to decrease the defects of products, improve the quality of products and shorten the time for processing, an analytical system of sheet metal numerical simulation is developed. It is a simulated numerical computation of the processing and forming process. The system can decrease the time for development and design, and reduce the cost of production. Besides, it can improve the optimization of quality and design of new products (You-Min Huang, Ching-Lun Li, 2008).

Formability of sheet metal is dependent on the mechanical properties of the material. A material that has the best formability for one stamping may behave poorly in a stamping of another configuration. Complex stamping require varying amount of stretching and drawing, to which bending, unbending, buckling and other complications are added. Most forming operations can be qualitatively, though not quantitatively, categorized as primarily stretching, primarily drawing, or varying ratios of each (R Cada, 1996).

The important material characteristics which determine the forming capacity of sheet metal are strength and ductility. Strength determines the size of the machinery needed for the forming process, while ductility determines the deformation a material can withstand without failure. In forming, ductility generally depends on the plastic properties rather than the fracture behaviour of materials, for ductile fracture occurs as a consequence of

prior localization of the deformation to form a neck. The plastic properties characterizing ductility are usually obtained from uniaxial tension tests(R Cada, 1996).

Recent research work in laboratories and press shops has shown that the forming capacity of sheet metal depends primarily on plastic anisotropy ratio r, which is the ratio of the strain in the width direction to that in the thickness direction and the strain-hardening exponent n. In drawing operations, r is of prime importance, while n is of lesser importance. In stretch-forming, however, the opposite is true. These two properties can be evaluated using a standard tension testing machine and normal tensile specimens (R Cada, 1996).

1.1 DEEP DRAWING

1.1.1 General description of the process

Deep drawing is a widely used name for a variety of processes by which a non flat product is made out of a flat sheet (called blank) in any other way then simple bending. Two groups of processes are generally distinguished: deep drawing and stretching. In pure deep drawing, the extra surface area needed for the product is obtained by pulling some material out of a reservoir called the blankholder area. In this process there is a movement of material in the plane of the sheet (not necessarily flat), and the whole art of deep drawing is to control this movement. In deep drawing tools three parts are distinguished: the die, the punch and the blankholder. The presence of this latter part, which is used for controlling the movement of the material, distinguishes deep drawing from simple stamping. For a cylindrical product the general construction of a deep drawing tool and the outline of the deep drawing operation is presented in fig. 1. The movement of the material out of the blankholder area is controlled by clamping the material between the die and the blankholder, the force used for this clamping is called the blankholder force. This clamping causes friction. In complex tools an extra control of the movement can be obtained by so called drawbeads.
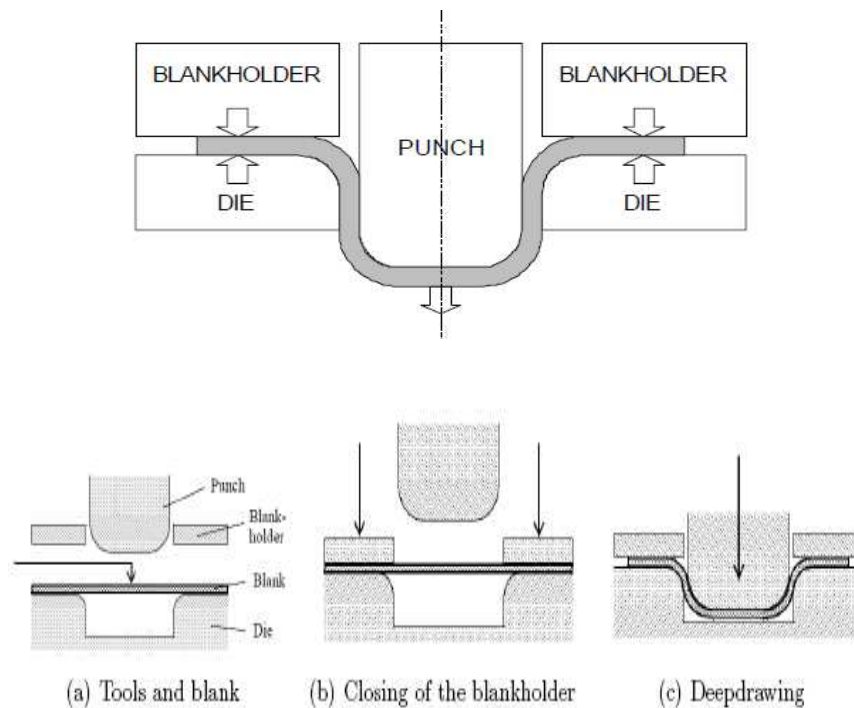
Fig. 1 Schematic representation of the deep drawing operation, for a cylindrical tool.

In fig.1 the area between the blankholder and the die is called the blankholder area, the material between the blankholder and the die is called the flange. The material being formed is clamped between the blankholder and the die by a clamping force (the blankholder force) and is pulled out of the blankholder area by movement of the punch (as shown in fig.1 c). In a stretching operation the material is completely clamped in the blankholder, the construction of the tool is otherwise similar to that of a deep drawing tool.

In pure stretching the extra surface needed for the product is obtained by stretching the material without any supply of fresh material. There are some basic differences between deep drawing and stretching. In deep drawing, the thickness of the material remains constant (in first approximation) while in stretching the material gets thinner (up to 50% in extreme cases). Furthermore, the contact in a deep drawing process is characterised by high speed of movement (equal to the punch speed) while in stretching the speed by

which the material moves against the tool is low. It should be clear that in a drawing operation of a complex shape both deep drawing and stretch type deformations occur.

Deep drawing and stretching are examples of sheet metal forming processes and are as such characterised by the facts that the deformation forces are oriented in the plane of the sheet, and that the surface pressures in the tool are generally (much) lower than the yield stress of the material. Other examples of sheet metal forming processes are bending, roll forming and spinning.

1.1.2 Friction conditions at deep drawing

In a deep drawing operation friction occurs as a result the material moving against the tool. In a traditional tool two areas of friction are distinguished: the blankholder area (simply called the blankholder) and the die radius. The third area which is sometimes mentioned, the punch radius, will not be considered in this work.
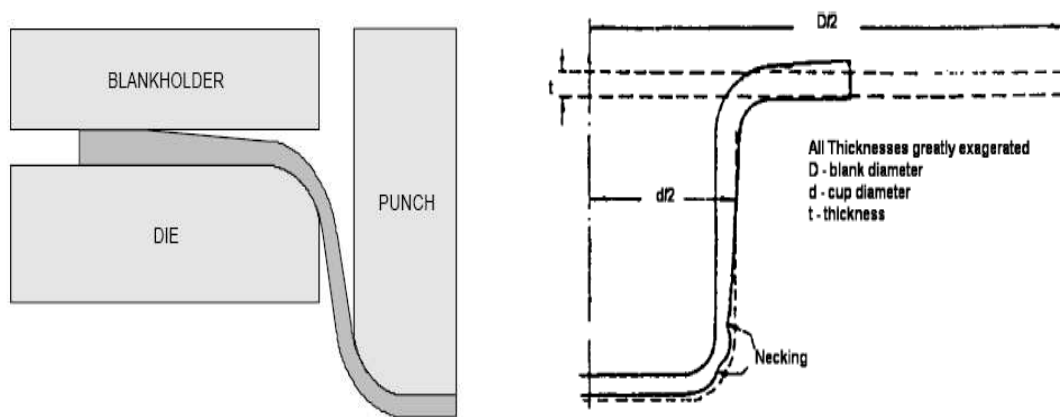

Fig.2. Variation in thickening of flange, deformation and necking of workpiece during deep drawing process (M. Colgan, J. Monaghan, 2003)

Fig.2 shows the typical shape characteristics and thickness variations of a partially drawn blank. Thickening occurs in the flange area and some stretching and necking occurs in the sidewall and just above the punch nose radius.

When the deep drawing operation starts, the blankholder closes and blankholder force is acting on the material. Initially, the material in the blankholder (the flange) is flat, so that the blankholder force is evenly distributed over the blankholder area. As the punch moves, the material is gradually drawn out of the blankholder area. This has some consequences. Firstly the surface area of the material in the blankholder decreases, so the average surface pressure on the material increases (assuming that the blankholder force is kept constant). However, due to the plastic deformation of the material in the flange, the material thickens at the outer edge as shown in the (fig 2). Consequently, the blankholder force is no longer evenly distributed over the flange but concentrates on the outer part. This thickening of the outer edge may become so strong that the sheet and the blankholder get separated and the inner part of the flange loses contact with the tool. In this way, the blankholder force is concentrated further on the outer part (fig 2). The sum of these effects is that the surface pressure on the places in the blankholder area where the friction force is generated increases significantly during the deep drawing operation. Initially, the type of contact in the blankholder is flat. Inspection of deep drawn parts reveals that in most practical situations the contact area in the blankholder remains flat. Only under extreme conditions, like very low blankholder forces or extremely thick material, the flange may wrinkle to such a degree that the blankholder force acts only on the tops of the wrinkles. Under normal conditions wrinkling can occur only in the inner part of the blankholder where the material loses contact with the tool (fig 2). In that situation the tops of the wrinkles may touch the tool, but only in extreme situations will these contacts bear a substantial part of the load. Experience shows that this only happens for relatively thick material. It is therefore safe to assume that in the blankholder friction is occurring at flat contacts.

It is very difficult, if not impossible, to actually measure the pressure on the outer edge of the flange during the deep drawing operation. At the onset of the operation the flange is still flat and the normal stress on the outer edge is equal to the mean stress. When the flange is being pulled inwards, the stress on the outer edge increases rapidly, indicating that the blankholder force concentrates on the outer part of the flange. When the stress on the edge exceeds twice the mean stress, the outer part has thickened so much that the

inner part fully loses contact with the tool. When the operation continues, the blankholder force will become more uniformly distributed, due to the increasing amount of plastic deformation in the material. For the die radius the situation is different. The material is bent over the die radius by the punch force which has to be transferred from the punch to the blankholder area. When the bending forces are neglected, the material will lie over the die radius like a membrane, and accordingly the contact is of conformal nature; the contact pressure is evenly distributed over the radius. However, in practice bending forces always occur. Recent simulations [Staeves 1996] show that the pressure gets concentrated in a few places, so that the type of contact is more like a line contact. The type of contact on the die radius can thus vary from conformal to line contact, largely depending on the ratio of material thickness to die radius.

The two main sources of friction in a deep drawing operation are the die radius and the blankholder area, at least for simple tools as pictured in fig 1. In practical situations, eliminating the friction at the die radius (if possible) will reduce the punch force by about 20%. Eliminating the friction in the blankholder area, however, may reduce the punch force by values of 50% or more.

1.1.3 Drawbeads

 The flow of the material during the deep drawing process is controlled by the blank holder geometry and the blank holder load. In order to increase the formability, these two aspects can be optimised. A widely used method to locally control the material flow is the application of drawbeads.

 Drawbeads are placed in the blank holder/die area. A drawbead consists of a bead attached to the blank holder or the die face. This bead fits into a groove or contra bead on the opposing face (fig. 3). The drawbead forces the blank material to bend and unbend several times while it is pulled through the bead. This bending and the friction generate a restraining force. By placing a drawbead wherever a restraining force is needed makes it a suitable tool to control the material flow.
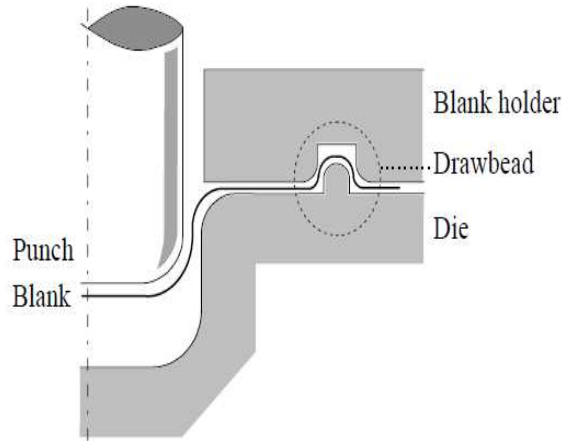
Fig.3 Drawing operation with Drawbead

1.1.4 Punch Force

In deep drawing operations the punch force is the force which is required to draw the material in to a die during forming operation, and is needed to draw the material under the blankholder plastically and to compensate for the friction there. Because the direction of movement of the punch is in general perpendicular to the direction of movement of the material in the blankholder, the force has to be 'bent' over 90°. This is done by drawing the material over the die radius, where an extra source of friction and deformation arises. In the discussion of the results of the deep drawing tests the relation between the punch force and the blankholder force is studied. Therefore the exact relation between the punch force and the blankholder force is of interest. The main sources of the punch force are the friction in the blankholder area, and the plastic deformation of the material being drawn. Neglecting bending forces and additional plastic deformation of the material over the die radius, the following expression for the punch force F_P can be written:

$$F_P = e^{\frac{\pi}{2} \cdot \mu_{die}} \cdot \left(F_B \cdot 2 \cdot \mu_{bl} + F_{def} \right) \cdot \frac{d_{punch}}{d_{bl,mean}}$$

$$= \quad A \quad \cdot \left(\quad B \quad + F_{def} \right) \cdot \quad C$$

7

Here μ_{die} is the coefficient of friction on the die radius, μ_{bl} the coefficient of friction in the blankholder, d_{punch} the punch diameter, d_{bl} the mean diameter of the area of the flange which is actually in contact with the blankholder, and F_{def} is the force needed for plastic deformation of the material in the blankholder area.

Part A accounts for the effect of pulling the material over the die radius (assuming that the material lies over the die radius like a membrane), part B is the actual friction force in the blankholder (the factor 2 stems from the two surfaces of the material).

There is a difference in speed between the punch (where the force is measured) and the material in the blankholder (the primary source of friction). While the total amount of work performed by the punch must be equal to the amount of work performed on the material in the blankholder, this difference in speed must be accounted for. The average thickness of the material remains more or less unchanged by the drawing operation, so the ratio of the speed can be taken equal to the ratio of diameters in part C. Assuming that the deformation force F_{def} is not affected by the blankholder force (this is true in first approximation), the derivative of the punch force F_P as a function of the blankholder force F_B can now be written as:

$$\frac{\partial F_P}{\partial F_B} = e^{\frac{\pi}{2} \cdot \mu_{die}} \cdot 2 \cdot \mu_{bl} \cdot \frac{d_{punch}}{d_{bl, mean}}$$

Assuming a value for the friction coefficient on the die radius of 0.15 (a common value), expression A becomes 1.26, while in practical situations expression C is 0.6- 0.9. So in first (and very rough) approximation we can assume that:

$$A.C \approx 1$$

We now introduce the term 'friction factor', defined as one half of the slope of the graph of the punch force – blankholder force relation (this terminology has been introduced originally by W. Van Merkenstein of Quaker Chemical). Using the above we now find:

$$\text{friction factor} = \frac{1}{2}\frac{\partial F_P}{\partial F_B} = e^{\frac{\pi}{2}\cdot\mu_{die}} \cdot \mu_{bl} \cdot \frac{d_{punch}}{d_{bl,mean}} \approx \mu_{bl}$$

The friction factor can be determined from the measured relation between punch force and blank holder force and is closely related to the coefficient of friction in the blank holder. In first, rough, approximation the friction factor is equal to that coefficient of friction. Therefore the friction factor can be used to study the friction in the blank holder area.

1.2 DESCRIPTION OF PROCESS VARIABLES

Significant factors which influence sheet metal forming include punch nose radius, die nose radius, clearance, blank holder, material properties and tooling and equipment.

1.2.1 Punch nose radius

In sheet metal drawing punch nose geometry is quite important since fracture mostly occurs nearer to punch nose radius. A sharper radius will require higher forces where the metal is folded around the punch nose and may result in excessive thinning or tearing at the bottom of the cup. To prevent excessive thinning, the punch nose radius (r_p) must be within the range of 4 to 10 times the metal thickness (t). If the radius of punch is less than four times the metal thickness, it may be necessary to form it over a larger punch radius and then restrike it to develop the specific radius. The radius may be determined by the product design when only one draw is necessary to complete the work piece because the cup bottom takes the shape of the punch nose. Experiments by Chung and Swift (1951) have shown that the punch nose radius was a major variable for determining limiting draw ratio. The empirical findings of the experiments of Hobbs and Duncan (1979) show that for $r_p \leq 2t$, the cup is highly failure-prone due to tearing while for $r_p \geq 10t$, stretching

may be pronounced. Further, it was also observed that within the region of $4t \leq r_p \leq 8t$, punch nose radius does not significantly affect limiting draw ratio.

1.2.2 Die nose radius

The die nose radius (r_{die}) depends on the thickness and size of the work piece. Theoretically, larger die nose radius reduces the draw load and increases the limiting draw ratio. However, if the draw nose radius is too large, it reduces the contact area between the flange and the blank holder and increases the tendency to wrinkle. Too sharp die nose radius will hinder the normal flow of the metal and cause uneven thinning of the cup wall, resulting in tearing. Smaller die nose radii may cause local failures in the bending zone by increasing the work hardening tendency. If the die nose radius is small, the interaction with the tools is also less which may cause a heat build-up, leading to the weakening of the die material and faster erosion. Mark Colgan and John Monaghan (2003) observed that the die nose radius is the most significant parameter influencing the drawing process. Slater (1977) observed that a safe region of the die nose radius can be identified for a given drawing process. It was also concluded that too much increase of the die nose radius does not significantly increase the limiting draw ratio and may lead to wrinkling or puckering. The experiments of Chung and Swift (1951) led to the conclusion that a safe region of $2t \leq rdie \leq 10$ was desirable in most of the sheet metal forming. The draw radius may be increased to 6 to 8 times the metal thickness when drawing shallow cups on heavy gauge metals without blank holder.

1.2.2 Blank Holder

The methods used for blank holding are clearance blank holding and pressure blank holding. Clearance blank holding maintains a fixed clearance which may resist anticipated thickening during drawing. Early work of Swift (1939) showed that with clearance blank holding, an initial clearance of 5% was sufficient for this purpose though the blank would thicken due to elastic deformation of tools. Swift (1939) also observed

10

that about 5% clearance does not avoid the development of stretching.

Pressure blank holding can provide a varying blank holding force and restrain the thickening of the flange. Pressure blank holding requires a double action die and is not integrated in a double stroke press. Swift (1939) observed that for pressure blank holding, higher blank holding force had little effect on the maximum punch load or on the final thickness on the base and the profile radius of the cup.

A blank holder plays very important role in drawing process, it prevent wrinkling of the blank when the cup is being drawn. There must be enough force on the blank holder to prevent the formation of wrinkles because when a wrinkle is initiated, the blank holder raises from the surface of the metal and allows wrinkles to generate. The blank holder force required to prevent wrinkling varies from practically zero in the case of the fixed blank holder to approximately one-third the drawing force. The blank holder pressure should be adjusted to a level just sufficient to prevent wrinkling of flange since the flange friction increases with blank holder pressure. Chung and Swift (1951) recommended a blank holder pressure of $1/2$ to 1 % of yield stress of blank material. Eary (1958) concluded that the optimum blank holder pressure decreases with increasing thickness (t) to diameter (d) ratio and the blank holder force is not required when $t/d \geq 0.25$. The force created by the blank holder also increases frictional forces. Very high blank holder force may create tearing on the sidewall of the drawn cup. The sidewall transmits the punch force to the area of the draw on the die radius. Tearing will generally occur near the punch radius because thinning is pronounced due to tensile forces. The different types of blank holders are shown in Fig. 4.
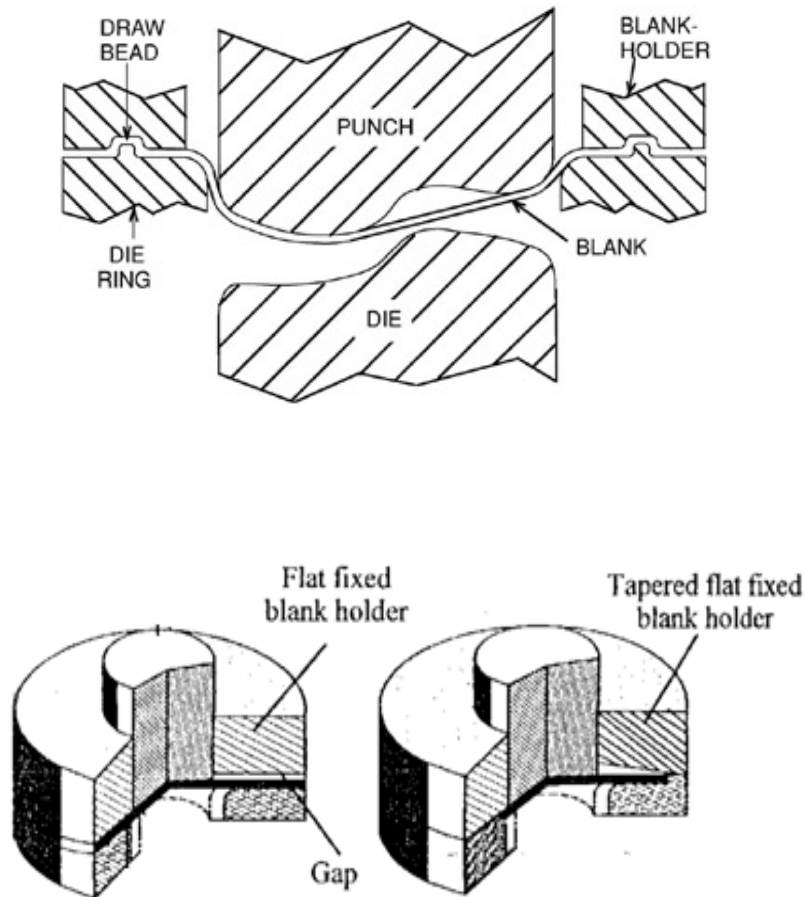
Fig 4. Different types of blank holders

1.2.4 Clearance

The clearance between the punch and die throat affects the flow region and geometry of the cup. The optimal clearance can be determined by two factors: material thickness and material type. For thinner material, the clearance should be as tight as possible to prevent ragged edges. However, for thicker material the clearance should be larger to allow the perforating process to be successful without damaging the punch and the die and to give a good edge quality (http://www.image2punch.com/Die-Clearance).

As the metal is drawn over the die radius, there is gradual decrease and then increase in the thickness of the metal. The draw force increases as the clearance decreases. A

secondary peak occurs on the force-stroke curve where the metal thickness is slightly greater than the clearance and where ironing starts. When clearance is equal to the metal thickness, ironing of the metal will occur near the top of the cup.

1.2.5 Material Variables

Flowstress, formability, anisotropy and microstructure are the important material variables in the analysis of the sheet metal forming for a given composition and deformation. Both flow stress and anisotropy influence the forming behavior. Further, they also affect the deformation behavior of the metal. Stretchability of metal is significantly affected by strain-hardening exponent (n) governing the neck strain distribution.

It was concluded by Whiteley (1960) that limiting draw ratio depends on normal anisotropy (r) **in** sheet metal as characterized by r-value. With r-value greater than unity, the flow stress in biaxial tension is raised relative to flow stress under tensile-compression system. The metal over punch head is straightened relative to metal in the flange and a greater draw ratio can be achieved. When drawing a high r-value metal, the thickness of the flange as it is drawn towards the die opening is less than for a low r-value metal and thickness of the resulting cup wall is uniform. Thus, for a given blank diameter, a deeper cup will result for a high r-value metal. Wilson et al (I965) reviewed the effect of n and r-values on draw ratios. Mellor and El-Sebaie (1972) has also reported the effect of n and r-value on limiting draw ratio while drawing with a flat headed punch. The microstructural features that determine the properties of the metal include the size, shape and orientation of the grains and their distribution. Generally microstructure consists of several grains connected together at grain boundaries. Each of the grains may have a random crystallographic orientation as the grains may have a preferred orientation. The mechanical properties are determined by the microstructure which contains one or more phases like martensite, ferrite, retained austenite and carbides in the case of steels. Depending on the nature of the phases and their volume fraction, high tensile strength can be achieved. The

desired microstructure is achieved by micro-alloying and thermo-mechanical treatment. A suitable thermo-mechanical treatment of –the whole sheet will improve the formability of sheet metals: A non-uniform or poorly textured microstructure in the sheet can cause poor deformation behavior and surface roughness in the formed component. Poor deep drawing behavior is manifested by excessive thinning, springback, orange peel and surface roughness.

1.2.6 Tooling and equipment

The selection of equipment for a given drawing process is quite influenced by the accuracy, load, energy characteristics and time. Optimum selection of the equipment requires consideration of the entire forming system including lot size, environmental effects, maintenance requirements as well as requirements of specific parts and process under consideration. Tooling variables include

- Design and geometry of punch and die
- Surface finish of tooling
- Stiffness of tooling
- Mechanical and thermal properties under condition of use

The forming severity of the localized region is mainly governed by tooling geometry and formability of the sheet metal.

CHAPTER 2

BEHAVIOUR OF MATERIAL IN SHEET METAL DRAWING

Sheet metal is deformed plastically to form the desired product. Many of the industrial products are either axisymmetrical or non-axisymmetrical shapes which are formed by press working. The deformation 15ehavior of sheet metal is greatly influenced by the forming techniques. Some of the fundamental tests such as tensile test and hardness test are used as a means of predicting the formability. Comparison of press performance with the data from tensile test, swift cup test and fracture analysis for rectangular shell was reported by Chung and Swift (1951 a, b). Further, the effect of deformation path on forming limit with respect to stretching under punch and flange was first discussed by Chung and Swift (1951a, b). Fracture limit analysis was attempted on shallow complex panels to identify the various aspects of drawing. Different defects created due to unbalanced distribution of stress and strain were monitored in the analysis.

2.1 FACTORS INFLUENCING PLASTIC DEFORMATION IN DEEP DRAWING

The important factors influencing the material behavior in sheet metal forming are the effect of planar anisotropy and work hardening coefficient. Amongst these factors, no single attribute individually relates with the deformation behavior of sheet metals for deep drawing. However, the tensile properties of sheet metal are generally used to assess the deformation behavior assuming that there is no appreciable change in stress-strain relation for various modes of deformation. Also, the deformation behavior of metal is influenced by the type of forming, forming geometry, forming speed, friction and lubrication.

2.2.1 Anisotropy value ($\bar{R}$) and work hardening coefficient (n)

The material behavior in sheet metal forming has been investigated widely to assess the press performance. No factor can be related individually with the deformation behavior of sheet metals. Some of the basic tests such as the tensile test and the hardness test were investigated in comparison with actual press operation as a means of predicting formability. Tensile test values have been used to evaluate the deformation behavior and press formability of sheet metal, on the assumption that there is no significant change in the stress-strain relation for various modes of deformation. The punch stretchability of sheet metal is its ability to biaxially elongate in the die cavity until a crack occurs on the blank. This property is strongly affected by the work hardening coefficient (n) governing the neck strain distribution. As the strain distribution depends mostly on the geometry of forming, the forming limit is significantly increased due to deep drawability of metal.

The work hardening coefficient (n) and the anisotropy value affect the magnitude of the limiting draw ratio. Sheet metal with good deep drawing characteristics should have a high r-value and small planar anisotropy. Sheet metal for combined forming by deep drawing and stretch forming should both have a high normal anisotropy value and a high work hardening coefficient. The bottom tearing force in deep drawn cups is also affected by the work hardening coefficient: A larger value of work hardening results in an increase in transferable load on deep drawn workpiece; a higher work hardening coefficient also means higher strain before necking. Depending on the type of forming process (deep drawing or stretch forming), the normal anisotropy (r) work hardening coefficient (n) will have a decisive role in determining the material behavior. Thus the limiting draw ratio increases with, increasing r-value and produces less thinning in transition region from cup bottom to the wall and also reduces the drawing load.

Yoshida and Miyauchi (1978) have observed that in the round bottom punch, stretching of metal under low lubrication, the strain level in the centre area surrounded by the hoop fracture is lowered as the n-value increases. This is because

for a lower n-value material, the centre area deforms more easily, being affected by the stress gradient in the earlier stages of forming. The effect of n-value on punch stretchability is the greatest when the fracture is observed at the top of a round bottomed punch under good lubrication. Deformation behavior in flat bottom and overhang regions is always in close relation with the n-value.
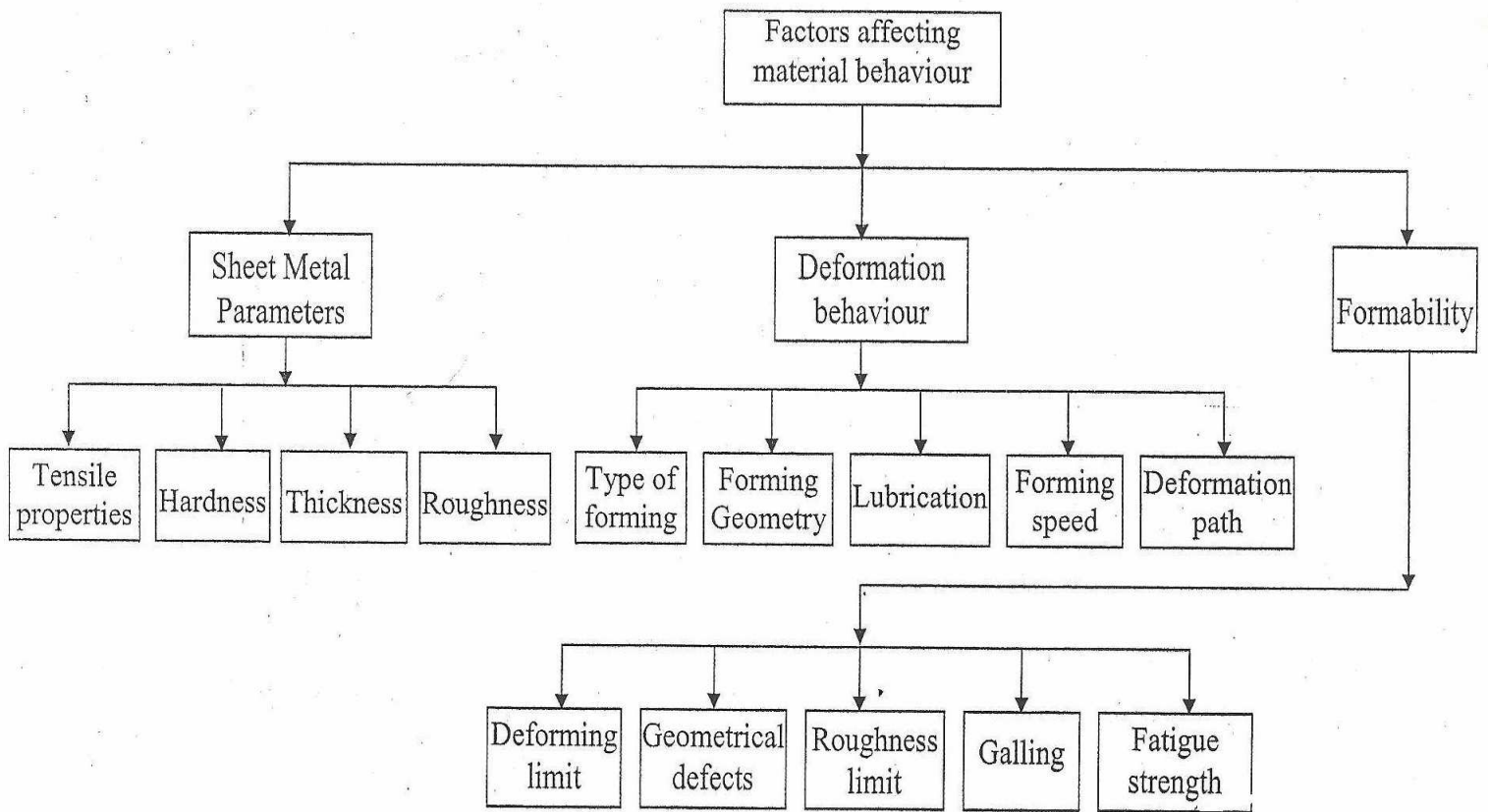

Fig.5   Factors affecting material behavior

2.2.2 Friction

At punch nose interface friction is an important factor for formability as it changes the strain path of critical site of the sheet in the forming limit diagram. Material parameters such as strain hardening and strain rate sensitivity are important for formability.

The deep drawability of the sheet metal can be increased by roughening the punch surface. Good lubrication and roughened punch surface may increase the draw ratio. Lower friction coefficients are used between the die and the blank to reduce heat formation and drawing force while higher coefficients are used between the punch and the blank to encourage uniform forming. During drawing, the elements on the blank moves upwards relative to punch causing shear stress between die and punch wall. Further, the bottom of the cup does not experience full drawing force and hence the bottom has not been work hardened compared to the wall of the cup. The drawing ratio may not exceed a certain value which depends on the characteristics of the metal, the shape of the draw, the ratio of the diameter to sheet thickness and the friction coefficient in the draw gap. Eshel et al (1986) have observed that friction at the punch bottom and nose is increased by increasing the surface roughness and by applying high pressure-resistant lubricants. The primary areas to be lubricated are the blank-die and blank-blank holder interface, blank-die comer interface, blank-punch interface and blank-punch head interface as shown in fig. 6
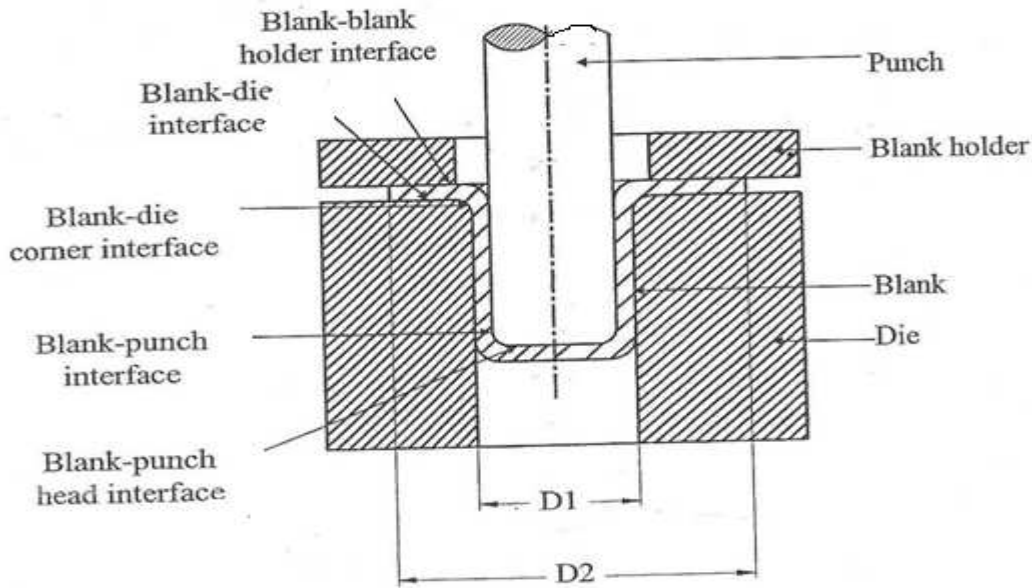
Fig. 6 Areas of lubrication in Deep Drawing

Lubricants used in deep drawing are thin fluid mineral oils, high viscosity lubricant film, emulsions and pastes. The thin fluid mineral oils are mainly used for deep drawing cold-rolled light gauge steel sheets which are used in automobiles. Thick oils, waxes or resins which provide high viscosity lubricant films are used for the more difficult drawing operations. Thickened oil like drawing greases are used on stressed parts of sheets along with fillers. The selection of lubricant depends on the ability to prevent the galling, wrinkling and tearing during drawing. It is also influenced by the ease of application, removal and corrosivity. Lubricants with high slip properties are applied to the blank and die surfaces prior to the drawing.

Granszow (1979) reported that the draw force transferred to the side of punch may aid in drawing into the die cavity and forcing the wall against punch. With low friction, there is increased tendency to thinning at cup bottom and failure region tends to shift into the punch nose radius. The lubrication is beneficial in the flange region of the cup as it reduces the work expended to overcome the friction.

2.2.3 Forming Speed

The punch penetrates the work piece at a certain velocity which has definite effect on the success of drawing operation. Slower drawing speeds must be used for lesser ductile metals. When excessive thinning occurs, the drawing speed must be reduced. The ideal conditions that have to be maintained to obtain optimum drawing speeds are the use of draw quality sheet metal, adequate lubrication, carefully controlled blank holder pressure and the condition of the press which are to be maintained at high level of accuracy. The punch speed in hydraulic press is relatively constant throughout the stroke. In mechanical presses, punch speed is taken as that at mid-stroke because the velocity changes in a characteristic manner throughout the drawing stroke from maximum velocity to zero. The drawing speed has greater influence in drawing stainless steel and heat resistant alloys than in drawing softer and ductile metals. Higher press speeds may cause cracking and excessive wall thinning while drawing metals with lower ductility.

Eary and Reed (1958) have observed that the change in punch velocity showed no significant change in punch force and limiting draw ratio. It was observed that defects such as wrinkling at the top and ripples in the side. wall of the cup are likely to occur. Meuleman (1980) also observed that the limiting draw ratio is independent of the punch speed. Avitzur (1982) has conducted analytical studies and observed that the punch force is independent of punch speed.

2.3 Failure modes in deep drawing

The limits of the sheet metal forming are determined by the occurrence of defects such as wrinkling and tearing on the blank. The limiting draw ratio is a measure of the limit in the drawing range. The failures in deep drawing are generally the undesirable geometry or surface finish of the cup. The most frequent types of failure are wrinkling, necking (tearing), scratching and orange peel.

2.3.1 Wrinkling

Wrinkling is a relatively common problem in deep drawing operations. It can lead to expensive redesign and remanufacture of tooling, lost press and operator time, and scrapped parts. The broad conditions under which wrinkling occurs are well documented (Avitzur, 1983). Depending on the relative intensity of lateral compression and axial tension, a workpiece may wrinkle elastically or plastically at a critical point during a drawing process. This condition is governed by a number of factors, most importantly, the geometry of tooling, specifications of the workpiece and drawing procedure. In general, unsupported regions of sheet or plate that are subjected to high compressive stresses are susceptible to wrinkling. For a given forming operation, however, prediction of the specific conditions that will result in wrinkling is a difficult task (Jamal Hematian, 2000).

There have been a large number of theoretical, experimental and numerical investigations of wrinkling in single step drawing of relatively thin sheet. Yu, Johnson and Stronge (1984) adopted an energy method to analyze plastic buckling or wrinkling of circular plates during spherical pressing (Jamal Hematian, 2000).
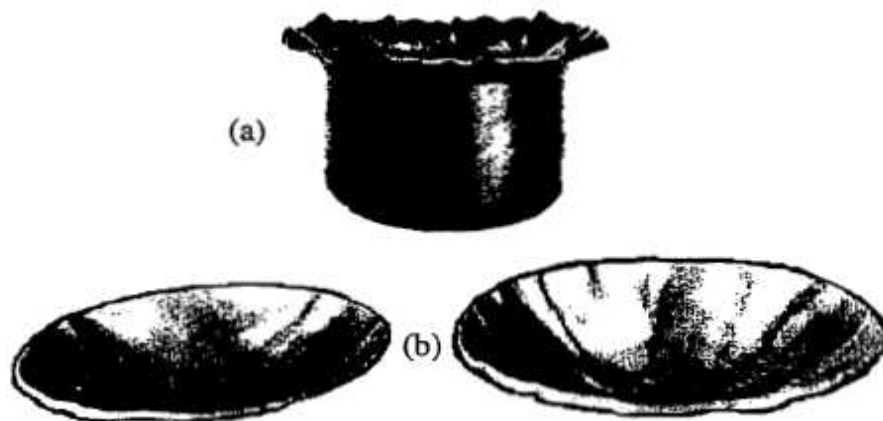

Fig. 7   Two samples of wrinkling ;(a) flange wrinkling,
(b) dish wrinkling (Jamal Hematian, 2000)

2.3.2 Tearing

In stretching of sheet metal over the punch, the rupture of the blank occurs over the punch nose profile .Necking precedes with eventual rupture. Hence, the forming limit is governed by the condition of instability and the site of necking initiation depends on the friction condition at the punch workpiece interface. Fig. 8 shows tearing (You-Min Huang, 2007)

Fig. 8   Tearing

2.3.3 Earing

The height of the walls of drawn cups usually have peaks and valleys as shown in Fig. 9 This phenomenon is known as earing. There may be two, four, or six ears, but four ears are most common. Earing results from planar anisotropy, and ear height and angular position correlate well with the angular variation of R. For two or four ears, earing is described by the parameter

$$\Delta R = \frac{R_0 + R_{90} - 2R_{45}}{2}$$

If ΔR>0, there are ears at $0°$ and $90°$, and if ΔR<0, ears form at $45°$. This variation is shown in Figure 9.

Earing is undesirable because the walls must be trimmed, creating scrap. With earing, the full benefit of a high R on LDR is not realized (Hosford and Cadell).
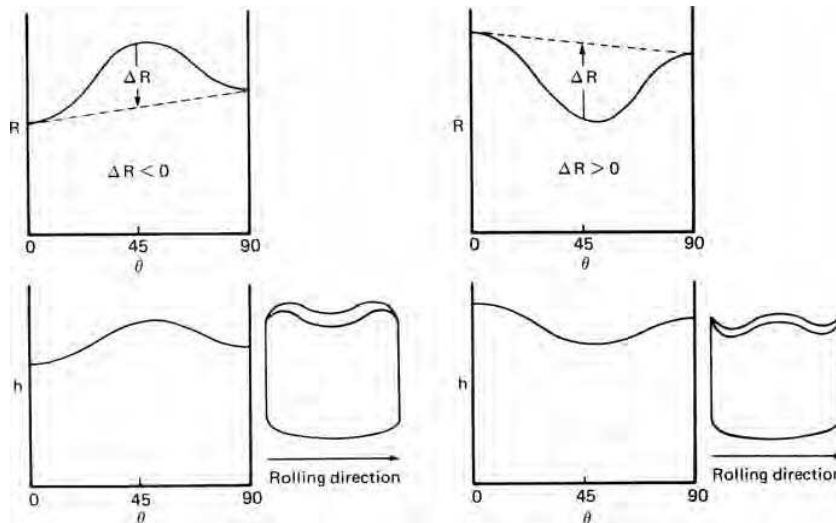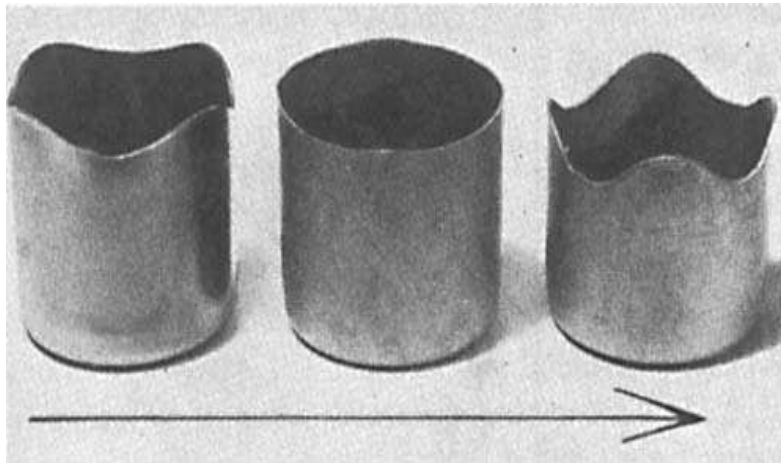

Fig. 9   Earing

2.4 Formability

Formability of sheet is often evaluated by simple tests such as a tensile test. The parameters obtained by simple tension, namely, degree of anisotropy, work hardening rate of stress-strain relation and maximum uniform elongation are related to formability. However, it is not possible to evaluate accurately the formability of metals in terms of these parameters. Thus for a complete assessment of the formability, the direct methods such as the Erichsen test and Swift cup test have been used for the determination of formability. Formability is the ability of a sheet metal to undergo stretching without necking or tearing. The scribed circle test of plastic instability and fracture in sheet metal forming was proposed by Keeler and Backofen (1963) to assess the formability of large-sized parts of very complex geometry like auto body panels. Yoshida and Miyauchi (1978) used scribed circle test for measuring the fracture strain. The deformation diagram can be obtained by the scribed circle test which shows the combined strain distribution and deformation path.

Quantitative assessment of formability is done by generating a forming limit diagram (FLD). Forming limit diagram can be generated either experimentally or by using analytical models and finite element simulations. Forming limit diagram is used to compare formability of different metals. Strips of metal of different widths, etched with small grid circles, typically 2.5 to 6 mm diameter, are tested with a very good lubricant over a spherical punch. A sheet wide enough to be clamped on all edges undergoes balanced biaxial tensile strain over the centre of the punch. As the width of the strip is decreased, the minor strain decreases. The minor strain may be positive or negative. The major and minor strains from the circle nearest to the tear can be considered to be a point on the boundary between safe and unsafe zones of the forming limit diagram. Forming limit diagrams are extensively used in predicting drawability. This avoids the limitations of analytical models by considering the resultant observations only. A curve which establishes the safe boundaries of strain can be drawn after observing a large number of tears and wrinkles, the material and

operational parameters. Since major stress in drawing is always tensile, the forming limit diagram shows that if the minor hoop stress is tensile too, thinning occurs. If the hoop stress is compressive, then thinning or thickening may occur. If both the stresses are compressive, the sheet will buckle. When the operating strains intersect the forming limit diagram, failure occurs.

CHAPTER 3

LITERATURE REVIEW

The literature review had been carried out to study the effect of various process variables, strain measurement techniques, numerical simulations and deformation behavior on the deep drawing process and identification of objectives.

A review of literature showed that earlier deep drawing process depended largely on trial and error. Many researchers tried to predict the draw forces by measuring the changes in thickness of a uniformly thick blank when drawn into a cylindrical cup. Chung and Swift (1951 a, b) conducted experimental investigations on cylindrical cups. Tendency for work hardening and reduction of thickness around the annular part was reported by Chung and Swift (1951a, b). Frictional forces were considered to be negligible and the material was assumed to be isotropic. Both plane strain and plane stress conditions were considered under Tresca yield criteria with the Levy-Mises flow rule. It was considered that generalized strain was equivalent to circumferential strain at the flange with friction at the rim of the blank. Experimental work of Chung and Swift (l951a,b) justifies these assumptions.

Chung and Swift's work (1951a,b) provided the basis for understanding radial drawing and thinning of the metal as it passes over the die. Chung and Swift (1951 a,b) reported the effect of punch load at different travel steps for materials like low carbon rimming steel, aluminium, brass and copper.

3.1 EFFECT OF WORK HARDENING AND ANISOTROPY IN DEEP DRAWING

The relationship between the deep drawability and r-values of sheet metals has been found by Keijiro Suzuki (1987) .He found that the r-value is related to the flange formation force alone and as it increased ,deep drawability was improved due to decrease in flange formation force. The wall strength of cup did not get much affected by the increased value of r.

The effects of factors such as tool geometry, material anisotropy, wrinkling, hardening are considered by Min Wan et al (2001) to formulate the fracture criteria theoretically which are expressed by the equations of limit stress and limit load during conical cup drawing based on stress-strain states in the critical section of fracture using Swift's instability criterion. He found that the limit stress and limit load depends on the material properties like r-value, n-value, tensile strength, semi-cone angle and punch nose radius. The increases in these values contribute to the improvement of the limit stress. It was concluded that the limit stress for the cylindrical cup was slightly lower than that of the conical cups.

The effect of mechanical properties on wall wrinkling in conical cups using cold-rolled and annealed stabilized steel, interstitial free steel and high strength low-alloy steel was studied by Jan Havranek (1977). He suggested that the material with a higher n and r-value and a lower yield stress generally provides wrinkle resistance.

3.2 EFFECT OF PROCESS VARIABLES IN DEEP DRAWING

The effect of deep drawing process of square and rectangular shells under different process conditions, using two different draw quality steels has been studied by Majlessi et al (1993a,b). The critical parameters such as shape, size of blank and tooling were examined. The results of these investigations were presented in terms

of punch load, through thickness and in-plane distribution, formations of flange wrinkles and fracture which were verified with experimental results. It was concluded that blank shape had a major impact on the strain distribution. This was due to the fact that cutting the corners of square and rectangular blanks led to a moderate deformation in the flange and consequently lower the punch load substantially. With a fixed blank shape, the punch load increased linearly with an increase in the blank size. It was observed that the increase of blank holder force delayed formation of visible wrinkles in the flange for larger punch penetrations.

The important factors influencing a drawing process, has been decided by Mark Colgan et al (2003) using design of experiments and statistical analysis. The punch and die radii, the punch velocity, blank holding force, friction and draw depth were varied and the results of the simulation and the experiments were compared. It was observed that the punch/die radii have a significant effect on the thickness of the deformed blank compared to blank holding force or friction. It was reported that for a smaller punch/die radii combination, the punch force will be more and the final draw will be shorter. Further, it was also observed that the die radius is the most significant parameter, followed by punch radius, draw depth and punch velocity. The blank holder force and lubrication have lesser effect on deviation in thickness.

The effect of material and forming characteristics on deep drawing of cylindrical and square cups using Explicit non- linear finite element code DYNA 3D for simulation has been studied by Mamalis et al (1997a,b). The numerical simulations were carried out by considering process parameters like punch velocity, sheet material density, coefficient of friction at the tool-blank interfaces and type and dimensions of finite element mesh elements and compared with experimental results regarding strain distributions (radial, circumferential and thickness through the sheet) and punch force-punch travel The evaluation of the CPU time cost, deformation modes, the strain distributions of the deformed material and the process parameters obtained for the finite element models were directed towards the selection of the most efficient material and punch parameters. It was reported that

the use of shell elements can reduce the CPU time cost by about 50%.

3.3 EFFECT OF BLANK HOLDING PRESSURE IN DEEP DRAWING

The effect of blank holding force on limiting draw ratio (LDR) while deep drawing circular magnesium alloy was studied by Shoichiro Yoshihara et al (2005). An improvement in the limiting drawing ratio was observed by providing the variable blank holding force during the drawing process, in comparison with the constant blank holding force conditions. It was reported that when the blank holding force is high, the experimentally drawn cup fractured at the wall part because of the low ductility of the material. The limiting draw ratio of the magnesium alloy sheet was observed to be improved using the blank holding force control technique and the results were verified by finite element method.

The influence of the elastic deflections of the blank holder on the pressure distribution between the blank holder and the sheet was analyzed by Leonid Shulkin et al (1996).He conducted a series of experiments and finite element method simulations and observed that variation of the blank holding force on the flange surface can be achieved by elastically deforming the blank holder in certain areas which results in improved control over the material flow resulting in a better deep drawn part. When a blank of uniform thickness is used and the blank holder surface is in close contact with the sheet, a slight deflection of the blank holder results in a significant change of the pressure; distribution on the blank holder sheet interface requiring relatively thicker steel blank holder.

The blank holding force over each node in the flange has been analyzed by Lung et al (1995). During the drawing process, when the nodal thickness in the flange reaches a critical value, the blank holding force and accordingly, the blank holding traction, were distributed such as to be assigned to the corresponding node according

29

to the suggested scheme of thickness consideration. Deep drawing of circular and square cups was analyzed by using the rigid-plastic finite-element method considering planar anisotropy.

3.4 EFFECT OF FRICTION IN DEEP DRAWING

The role of friction in metal forming with particular reference to energy saving in deep drawing was investigated by Plevy (1980). The presence of a solid polymer film lubricating barrier during deep drawing can significantly reduce the drawing energy requirement of precoated metal sheet at low tooling clearances. The polymer film has been reported to be very effective in keeping the surface integrity of the coated sheet. Significant reductions in asperity height were observed when oil lubrication was employed while PTFE film lubrication helped to maintain asperity height.

Tsung-Sheng Yang (1999) developed an analytical model to check the effect of friction on strain distribution for full film lubrication and dry friction condition of deep drawing by combining the elastic-plastic membrane finite element code of deep drawing together with full film lubrication theory. The film thickness and the strain distribution of full film lubrication are predicted. It was observed that the theoretical results agreed reasonably well with the experimental results.: The strain distribution in the full film lubrication has been compared with the dry friction condition and it was concluded that the strain distribution in the full film lubrication region is more uniform. It was also observed that the drawability in the full film lubrication is better than the unlubricated condition.

Bilgin Kaftanoglu (1973) observed that lubrication affects the boundary frictional stresses and modifies the strain distribution across the cup. It was observed that the location of plastic instability and fracture and the magnitude of the instability or fracture strains in deep drawing depend largely on the conditions of lubrication between the sheet metal and tools. The friction coefficients in

stretch forming were found to be much higher than those in radial drawing. The experimental results indicated that the plastic films (PTFE) could be more effective in reducing friction than grease type lubricants. It was observed that the coefficient of friction for the grease lubricants decreased with the increasing deformation.

3.5   FINITE ELEMENT ANALYSIS IN DEEP DRAWING PROCESS

The geometric non-linearity in rigid-plastic finite element formulation· of continuum elements for large deformation during an incremental time step has been considered by Lee and Yang (1997). In sheet metal deformation, the displacement for each step is considered large even though the effective strain increment is very small. For such large displacement problems, geometric non-linearity was considered.

The effectiveness of implicit, explicit and iterative implicit/explicit finite-element analysis methods has been compared by Yang et al (1995) for the analysis of static and dynamic sheet-forming problems. The rigid-plastic finite- element method using both the usual membrane elements and bending-energy-augmented membrane elements (BEAM) was considered for analysis. Computations were carried out for some typical sheet-forming process by implicit, explicit, iterative implicit/explicit schemes, including deep drawn components.

Hematian (2001) used finite element-based models to investigate the effect of initial tooling imperfections on the initiation of wrinkling in deep drawing of thick sheet. Major tooling imperfections such as punch displacement and blank tilting were considered. The simulation results were compared qualitatively with experimental study. The results show that the finite element method indicates that for a thick plate, punch displacement has negligible effect on the initiation of wrinkling while blank tilting is a critical parameter.

3.6 EXPERIMENTAL STUDIES IN DEEP DRAWING

Sosnowski et al (1992) conducted a comparative study on sheet metal forming process by using both numerical simulation and experimental study. Tests were conducted on circular and rectangular blanks with cylindrical and prismatic dies. Strain and thickness distribution have been measured after each test. Different friction coefficients were used with both lubrications and dry conditions on the tool and blank interfaces. The error between the experimental values and the results of calculations of strain was relatively small.

Claudio Garcia et al (2005a) presented the numerical modeling and experimental validation of deep drawing of EK4 steel sheets for three different deep drawing applications: the Erichsen test, a cylindrical cup test and an industrial sheet metal forming application of deep drawing of the lower component of commercial washing machine. A finite element analysis of the deformation process was performed with a large strain hyper elastic shell formulation including the Hill-48 associate plasticity model. The mechanical interactions between the sheet and the different tools (punch, blank holder and die) were taken into account through a Coulomb-type contact friction law. A constant blank holding force was assumed during the forming process in each case. The punch force together with the in-plane principal deformations and thickness strain distributions of the final deformed part were validated with experimental results which were found to be satisfactory.

Zaky et al (1998) proposed studies to determine the optimum shape of the blank for deep drawing of low carbon steel without ears. The earing behaviour of the deformed cup was predicted from the anisotropic properties of the sheet metals. Lubrication was provided on both sides between the die and blank holder. It was also observed that ears are formed in the direction of normal anisotropy (r) where it is maximum.

3.7   OBJECTIVES AND SCOPE OF THE STUDY

The specific objectives of the work are identified as:

1. Characterization of tensile properties and forming parameters of CRDQ steel.
2. Experimental determination of material parameters i.e. anisotropy, strain hardening coefficient and thinning.
3. Development of correlation between limit strains and material parameters.
4. Prediction of failure in CRDQ steel (using simulation software HW Radioss) at different blank size, blank holding pressure & die corner radius.
5. To compare the results determined experimentally with software analysis

CHAPTER 4

FINITE ELEMENT ANALYSIS OF DEEP DRAWING PROCESS

4.1   INTRODUCTION

The FEA or Finite Element Analysis is an applied technique in engineering that aims to evaluate the functionality of a certain product design before the prototypes are produced. This discipline is being observed by different industries such as the car and aircraft companies. It actually became an important aspect in the production of materials because of its usefulness and dependability. Numerical solutions to even very complicated stress problems can now be obtained routinely using FEA [David Roylance, 2001].
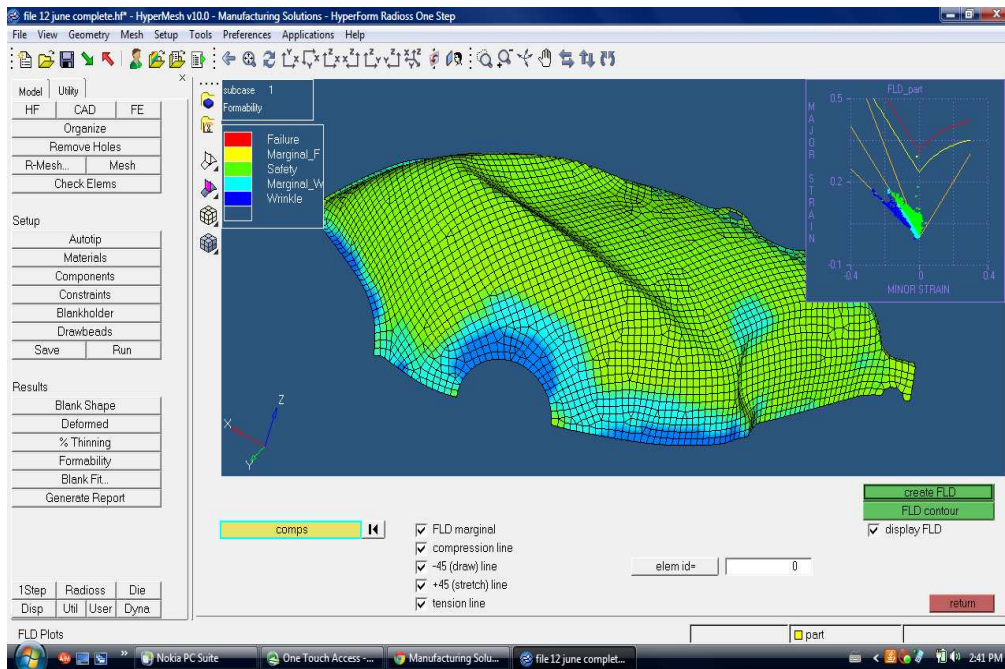
Fig.10   FEA in HyperMesh

While the Finite Element Analysis seems to be a little complicated for the untrained eye, product developers and big industries have relied on this assessment technique in order to save time, effort and money. The production of various automotive sheet parts is now streamlined and cost-effective. Here are some of the advantages that can be gained from implementing this analysis:

- Helps in Prototype Improvement – Based on the analysis, the product can be improved or modified in order to suit the requirements of the real world. The FEA can suggest changes to match the existing standards of production.
- Saves Time, Effort and Money – Because the failure in the model is easily predicted through FEA, the cost of producing prototypes is reduced. Also, it tends to minimize the time and effort required for conceptualizing a product since every model can be redesigned accordingly.
- High-Quality Product – Having undergone some scrupulous analyzations, the product achieves a superior quality that is suitable for practical application. The modifications that are suggested by the Finite Element Analysis will help the developers improve their product.
- Increased Production Rate – Due to the time saved through the careful assessment of the model, the manufacture of the products is likely to flow seamlessly. With FEA, the developers can guarantee the quality of the products before they are presented to the market.
- Ensured Safety – With FEA, the stresses on the product can be easily detected   even before the actual testing. It conveniently points out the possible failure in the model. Because of this, the prototypes are redesigned to comply with the standards of the practical applications. The final products are therefore safe and efficient just as they were initially tested.

In spite of the great power of FEA, the disadvantages of computer solutions must be kept in mind when using this and similar methods: they do not necessarily reveal how the stresses are influenced by important problem variables such as materials properties and geometrical features, and errors in input data can produce wildly incorrect results that may be overlooked by the analyst. Perhaps the most important function of theoretical

modeling is that of sharpening the designer's intuition; users of finite element codes should plan their strategy toward this end, supplementing the computer simulation with as much closed-form and experimental analysis as possible [David Roylance, 2001].

4.2   CONSTITUTIVE EQUATIONS

A number of finite element analyses for modeling sheet metal forming process have been reported in literature during the last ten years. According to the constitutive equations used in process modeling, the finite element method can be grouped into typical categories. These are rigid-plastic analysis and elastic-plastic analysis. Either approach may incorporate various effects by means of flow stress that depends on strain rate.

4.2.1   Elastic-plastic model

Elastic-plastic programme can treat the transition point and elastic response in an approximate way in order to speed up computation and allow for larger steps. Elastic-plastic model can model both elastic and plastic response of material with the possibility to predict springback which is mainly an elastic bending effect upon unloading. The penalty is that the elastic-plastic constitutive equation is usually formulated in a rate form and small time steps must be taken in order to make a good approximation of the elastic behavior, particularly to the transition between loading and unloading element.

In the elastic-plastic analysis, the linearity in stress-strain relation leads to a system of incrementally linear equations amenable to direct solution technique for calculating nodal displacement rates and strain rates. As the sheet metal forming process involves both material and geometrical non- linearities, the step size required for accurate integration is necessarily small.

4.2.1.1   Formulation for elastic-plastic deformation

The different types of elements used for finite element analysis arc linear elements, plane-strain triangular elements, linear quadrilateral elements and higher-order quadratic elements and three-dimensional elements. The accuracy of the finite element solution improves as the number of elements is increased. The number of elements is normally limited by the size of the computer memory and the time for solution of the simultaneous equations.

In metal forming analysis, the deforming loads are not known initially while the components of displacement of certain nodes will be determined by the boundary conditions of the problem. Even though the applied nodal forces are not known, the resultant forces will be known at many nodes mainly inside the body and on the free surfaces of the work piece. At these nodes, resultant force is zero and the displacement must be determined. Generally at the start of the analysis, most of the components of the global nodal force vector (t) are known to be zero. The components of the global nodal displacement vector (d) will be specified by the boundary conditions of the problem.

The strains in plastic deformation are very large and even though the deformation involves only a small amount of plastic strain, the yield stress will change in a non-linear manner. The metal deforms elastically at first with constant values of Young's Modulus and Poisson's ratio, but as soon as the stress reaches the yield value, plastic deformation occurs with a much lower effective modulus. The yield stress itself increases with strain due to work hardening and stress is no longer proportional to strain but is related to the strain increment and the strain rate.

4.3 Yield criterion

The problem of deducing mathematical relationships for predicting the conditions at which plastic yielding begins when a material is subjected to any possible combination of stresses is an important consideration in the field of plasticity. It is expected that yielding under a situation of combined stresses can be related to some particular combination of principal stresses. There is at present no theoretical way of calculating the relationship between the stress components to correlate yielding for a three-dimensional state of stress with yielding in the uniaxial tension test (George E. Dieter).

Yield criterion is used to specify the critical or yield stress at which the metal begins to yield. The yield criterion is generally expressed as a function of the yield stress invariants as below.

$$F (J1, J2, J3) = A \ (\text{constant})$$

where A refers to the strength coefficient and J1, J2 and J3 refers to the first, second and third stress invariants respectively and are given by

$$J1 = \sigma ij$$
$$J2 = \tfrac{1}{2}(\sigma ij \sigma ij - \sigma ii \sigma ii)$$
$$J3 = | \sigma |$$

4.3.1 Tresca's Yield Criterion

According to Tresca's yield criterion the material begins to yield when the maximum shear stress exceeds a critical value, called shear yield stress (τy). If the principal stresses are σ1, σ2, σ3 where σl > σ2 > σ3, then yielding criterion is generally expressed as a function of the principal stress as below

$$\sigma 1 - \sigma 3 = f (A)$$

For the case of pure shear, σ1 = -σ3, and σ2=0.

4.3.2 Von Mises Yield Criterion

Von Mises proposed a symmetrical quadratic condition

$$(1/\sqrt{2}) \, [(\sigma_1 - \sigma_2)^2 + (\sigma_2 - \sigma_3)^2 + (\sigma_3 - \sigma_1)^2] = A \text{ (constant)}$$

where, σ1, σ2,σ3 are principal stresses in x, y and z directions.

This includes all three principal stresses. According to this criterion, the plastic flow occurs when the shear strain energy exceeds a limiting value. The shear strain energy per unit volume can be expressed in terms of principal stress as

$$\text{Shear strain energy} = (1/6G) \, [(\sigma_1 - \sigma_2)^2 + (\sigma_2 - \sigma_3)^2 + (\sigma_3 - \sigma_1)^2]$$

Where G is the shear modulus.

4.3.3 Hill's Anisotropic Yield Criterion

During the plastic deformation at room temperature, the mechanical properties of metal may vary in different directions and this property is called anisotropy. Hill's theory will be used to describe the state of anisotropy, when there are three mutual orthogonal planes of symmetry at every point. Hill's potential function is a simple extension of the Von Mises function, which can be expressed in terms of rectangular Cartesian stress components as

$$f(\sigma) = \sqrt{F(\sigma_{22} - \sigma_{33})^2 + G(\sigma_{33} - \sigma_{11})^2 + H(\sigma_{11} - \sigma_{22})^2 + 2L\sigma_{23}^{\,2} + 2M\sigma_{31}^{\,2} + 2N\sigma_{12}^{\,2}}$$

where F, G, H, L, M and N are constants obtained by tests of the material in different orientations.

4.4 FINITE ELEMENT ANALYSIS SOFTWARES

4.4.1 Dynaform

Dynaform software is an LS-DYNA-based sheet metal forming simulation solution package. Dynaform's analysis engine is LS-DYNA, it is a general purpose, non-linear, dynamic, finite element analysis code utilizing explicit and implicit capabilities for solving fluid and solid structural problems. The software has been developed for applications such as automobile crashworthiness, occupant safety, underwater explosion, and sheet metal forming.

4.4.2 Hypermesh

Altair HyperMesh is a high-performance finite-element pre-processor for popular finite-element solvers. It allows engineers to analyze product design performance in a highly interactive and visual environment. Advanced functionality within HyperMesh allows users to efficiently manipulate geometry and mesh highly complex models. Advanced functionality within HyperMesh allows users to efficiently manipulate geometry and mesh highly complex models. These functionalities include extensive meshing and model control, morphing technology to update existing meshes to new design proposals and automatic mid-surface generation for complex designs with varying wall thicknesses. Solid geometry enhances tetra-meshing and hexa-meshing by reducing interactive modeling times, while batch meshing enables large scale meshing of parts with no manual clean-up and minimal user input.

CHAPTER 5

METHODOLOGY

The methodology followed in this work is explained below in two different sections: experimental work and FE analysis.

5.1 Experimental work:

The experimental work carried out for determining the tensile properties, formability parameters, limited dome height and forming limit strains of CRDQ steel are explained in this section.

5.1.1 Selection of materials

Composition and different material properties of CRDQ steel used for experimental work are given in Table 1.

Table 1: Chemical composition of the CRDQ steel used (by weight %)

ASTM E-1507												
Elements	Fe	C	Si	Mn	Ni	Cr	Mo	Cu	V	Al	Ti	S	P
% Conc.	99.56	0.053	0.018	0.076	0.039	0.037	0.053	0.022	0.036	0.018	0.045	0.020	0.016

Table 2: Different Mechanical properties of CRDQ steel

UTS (N/mm^2)	Yield Stress(0.2% Proof Stress) (N/mm^2)	EL%	Hardness(HRB)	Anisotropy (r)	Strain hardening coefficient (n)
244.34	138.9 N/mm^2	44.20	69-70	1.5	.24

CRDQ sheets of same grade and thickness were used to study the effect of blank holding pressure on the FLD.

5.1.2 Determination of tensile properties
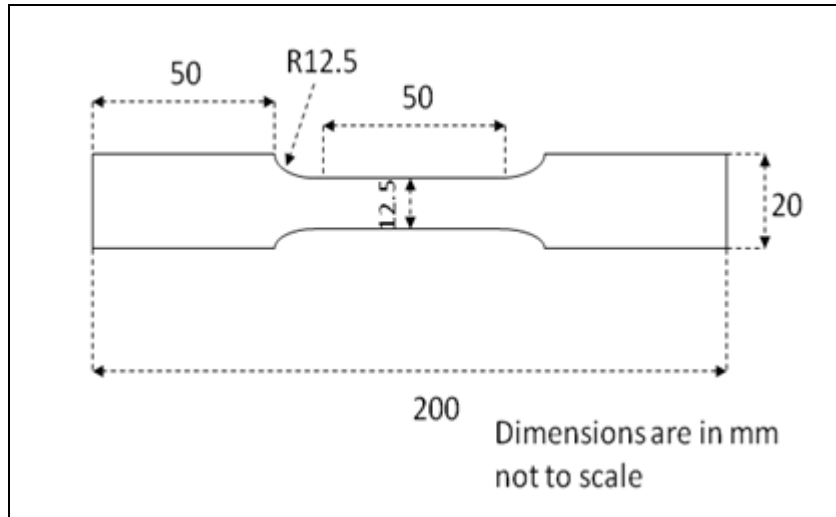
Fig. 11: Dimensions of Tensile specimen (ASTM E8)

Tensile tests were carried out using specimen machined as per ASTM standard E8M specification as shown in fig. 11. The specimens were tested along the three directions, with the tensile axis being parallel (0^0), diagonal (45^0), and perpendicular (90^0) to the rolling direction of the sheet (D. Ravi Kumar,2002).

Fig. 12: 10 Ton Instron machine used for tensile testing

The specimens were tested in uniaxial tension on Instron machine (Fig. 12) at a constant cross head speed of 5 mm/min. The tested and untested tensile samples are shown in Figure. Load elongation data was obtained for all the tests which were converted into engineering stress strain curves. The standard tensile properties such as yield stress, ultimate tensile stress, uniform elongation and total elongation were determined from the stress- strain data.

The point corresponding to max stress was taken as the UTS and the stress at 0.2% offset was taken as the YS. The total elongation was measured using an initial gauge length of 50 mm.

The strain hardening behavior can be described using the Holloman's equation.

$$\sigma = K\varepsilon^n$$

Where σ=true stress, ε=true strain, n=strain hardening exponent, K=strength coefficient. For determining the n value of these sheets, the engineering stress strain data were converted into true stress-true strain curves using the following equations.

$$\sigma = s(1 + e)$$
$$\varepsilon = \ln(1 + e)$$

Where s = engineering stress and e= engineering strain.

The log true stress and log true strain values were calculated in the uniform plastic deformation range (between YS and UTS) and using linear regression (least square method) a best fit was plotted. The slope of this line gives n value and Y- intercept gives log K.

5.1.3 Determination of average plastic strain ratio (Normal anisotropy – $\bar{R}$ value)

The plastic strain ratio, which is a measure of anisotropy, was determined using specimens prepared according to ASTM specification. The specimens were elongated to predetermined longitudinal strain (10% and 15%depending on the % elongation up to UTS) and the testing was stopped before the onset of necking. Final width and gauge length were measured and the plastic strain ratio (R) is calculated as below [George E Dieter, Mechanical metallurgy].

$$R = \frac{\varepsilon_w}{\varepsilon_t} = \frac{\varepsilon_w}{-(\varepsilon_w + \varepsilon_l)} = \frac{\ln\frac{w_f}{w_0}}{\ln\frac{l_0 w_0}{l_f w_f}}$$

W_0, l_0: initial width and length, W_f, l_f: final width and length

ε_w=true width strain

ε_t=true thickness strain

ε_l=true length strain

The R value was determined in three directions as mentioned in the tensile tests by repeating the above procedure. The normal anisotropy or average plastic strain ratio was calculated using the formula ($\bar{R}$):

$$R_{avg} = (R_0 + R_{90} + 2R_{45})/4$$

R_0, R_{45} and R_{90} represent the R value in three directions.

Calculations of Anisotropy:

Table 3   Value of variables at different positions

Variables	Sample 1(mm) 0^0	Sample 2(mm) 45^0	Sample 3(mm) 90^0
W_f	11.18	11.624	11.34
W_o	12.23	12.57	12.426
L_f	57.31	57.94	57.74
L_0	50	50	50

From above:

$R_0 = 1.92$

$R_{45} = 1.167$

$R_{90} = 1.757$

$\overline{R} = 1.5$

Stress and strain calculations

Table 4   True Stress – True Strain values from Tension Test

Elongation(mm)	load(KN)	Engg stress(Mpa)	Engg strain	True Stress(Mpa)	True strain
3.5	0	0	0.07	0	0.067659
4.9	2.4	112.2544434	0.098	123.2553789	0.09349
6.09	2.96	138.9	0.1218	155.81802	0.114935
7	3.04	142.1889616	0.14	162.0954163	0.131028
9.1	3.36	157.1562208	0.182	185.7586529	0.167208
11.2	3.68	172.1234799	0.224	210.6791394	0.202124
14	4	187.090739	0.28	239.4761459	0.24686
16.8	4.08	190.8325538	0.336	254.9522919	0.28968
19.6	4.16	194.5743686	0.392	270.847521	0.330742
22.4	4.4	205.7998129	0.448	297.9981291	0.370183
25.2	4.48	209.5416277	0.504	315.150608	0.408128
29.4	4.8	224.5088868	0.588	356.5201123	0.462475
33.6	4.8	224.5088868	0.672	375.3788587	0.514021
36.4	4.8	224.5088868	0.728	387.9513564	0.546965
40.6	4.88	228.2507016	0.812	413.5902713	0.594431
42	4.88	228.2507016	0.84	419.9812909	0.609766
44.8	4.96	231.9925164	0.896	439.857811	0.639746
47.6	5	233.8634238	0.952	456.5014032	0.668854
49	5	233.8634238	0.98	463.049579	0.683097
50.4	4.96	231.9925164	1.008	465.8409729	0.697139
51.8	5.08	237.6052385	1.036	483.7642657	0.710987
54.6	5.2	243.2179607	1.092	508.8119738	0.738121
56	5.2	243.2179607	1.12	515.6220767	0.751416
57.4	5.224	244.3405051	1.148	524.8434051	0.764537
59.5	5.2	243.2179607	1.19	532.647334	0.783902
61.6	5.2	243.2179607	1.232	542.8624883	0.802898
63	5.04	235.7343312	1.26	544.102976	0.815365
63.7	4.88	228.2507016	1.274	548.309875	0.82154
64.4	4	187.090739	1.288	554.409865	0.827678
65.1	3.92	183.3489242	1.302	560.574893	0.833778
65.8	3.68	172.1234799	1.316	562.355634	0.839842
66.5	3.36	157.1562208	1.33	564.355674	0.845868
67.2	3.2	149.6725912	1.344	566.234556	0.851859

UTS = 244.34 Mpa, Y.S = 138.9 Mpa
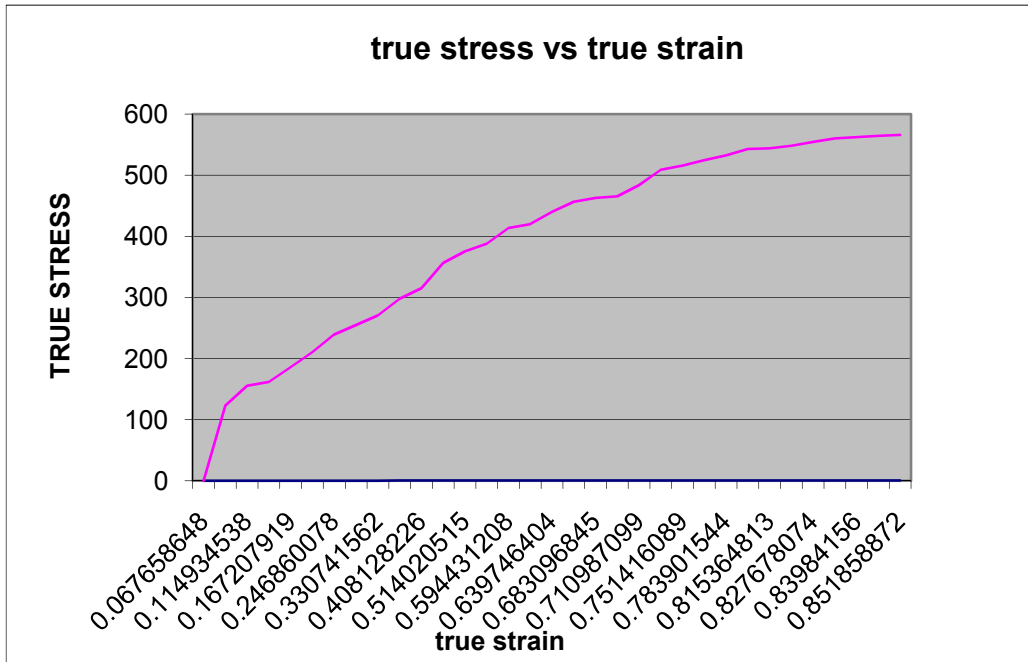
Fig. 13 True Stress-True Strain curve

5.2 Testing the material for biaxial stretching:
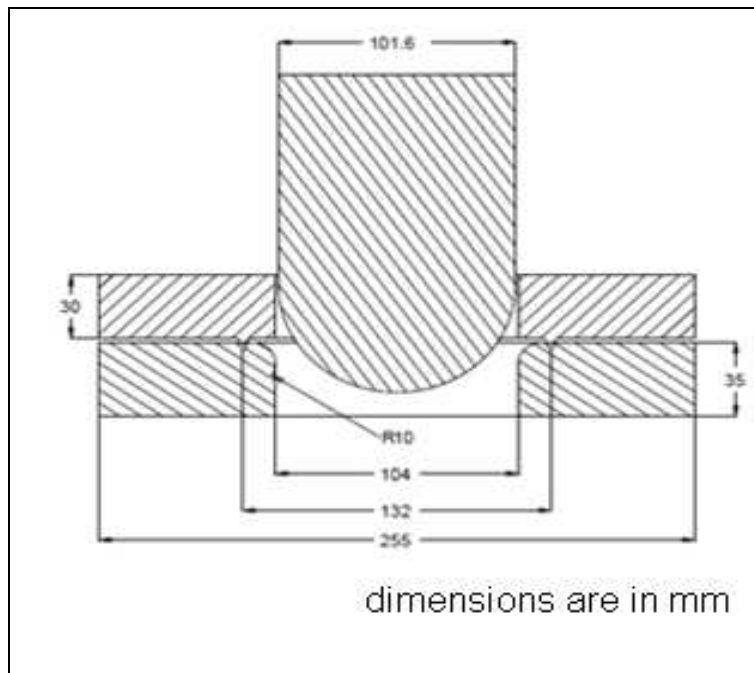
Fig. 14 : Schematic of punch and die setup for LDH tests

47

A 101.6 mm diameter punch was used with dies (lower die and blank holder) having a draw bead to prevent the drawing in of the blank for certain widths. The draw bead ensures that only portion of blank within the die region is stretched completely without drawing. The sheet strip was clamped firmly between the die and the blank holder before it gets stretched over the punch. In the current setup the draw bead diameter is 132 mm. The blank was cut with length perpendicular to the rolling direction. The blank was stamped with 5mm diameter circles with a gap of 0.5 mm between the circles as shown in figure. A typical Stamped CRDQ steel specimen is shown in Fig. 15.
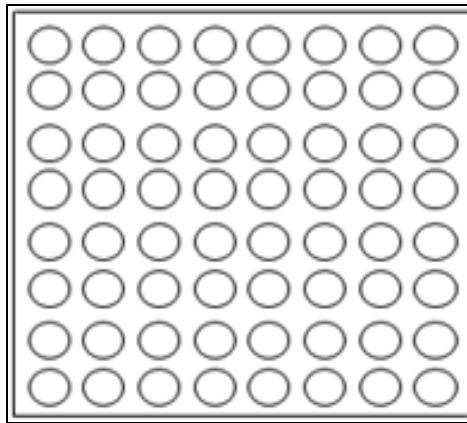
Fig. 15: Pattern of grid marking on the samples

5.2.1 PREPARATION OF THE BLANK

The test specimens of square-shaped blanks of CRDQ steel were prepared by blanking. The geometrical parameters of the blank like trueness, flatness and uniformity of the metal thickness were checked to homogenize the blank for deep drawing experiments. Hemispherical cups were deep drawn from square blanks of 175 X 175 mm. The test specimens were stamped with 5 mm diameter grid circles for determining the strain distribution in the cups. The grid circle diameters were inspected for their uniformity using a Tool Maker's microscope. Fig. 16 shows the view of the stamped

square blanks.
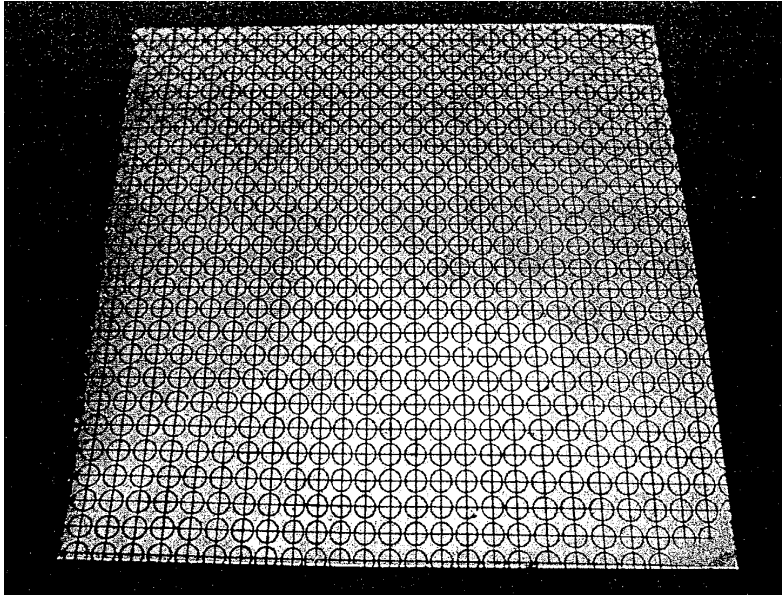
Fig. 16   Pattern of stamping on the sample for LDH test

5.2.2 Stretch forming experiments

The grid marked specimens were deformed using a double action hydraulic press of 100-tonne capacity. A view of the experimental setup mounted on the hydraulic press is shown in Figure. 17

Fig. 17 Experimental setup on the 100-tonne hydraulic press

The specimen was placed between the upper and the lower dies. An optimum blank holding force in the range of 1-1.5 tonnes was applied on the upper die to clamp the blank at the draw bead. The experiment was stopped when a visible neck or initiation of fracture was obtained on the specimen. In all the above stretch forming experiments a data acquisition system consisting of a load cell and a rotary encoder was used to obtain the load - displacement data during the experiments. Amplifier was used to amplify the signals from the load cell and the rotary encoder. These amplified signals are converted to digital signals by analog to digital converter and fed to the computer. From these digital data, a load - displacement curves were plotted.

5.2.3   Strain measurement

Major and minor principal strains were calculated by measuring major and minor diameters of ellipses on the deformed samples. A travelling microscope having a least count of 0.001mm was used to measure major and minor diameters of ellipses for strain calculations. A picture of travelling microscope used is given in fig. 19

Fig. 18 Specimen with Necking

Fig 19 Travelling Microscope used for measuring deformed circles.

Major axis(mm)	Minor axis(mm)	Major strain (%)	Minor strain (%)
8	5.9	60	18
8.1	5.4	62	8
8.2	5.92	64	18.4
8.5	5.45	70	9
8.56	5.76	71.2	15.2
8.7	5.5	74	10
7.6	5.29	52	5.8
7.5	5.58	50	11.6
7	5.52	40	10.4
7.2	5.62	44	12.4

Table 5. Major and Minor strains

5.2.4 Cup Height measurement

The limited dome height (LDH) of specimen at the point of necking/fracture was measured using a vernier height gauge with a least count of 0.02 mm.

LDH = 39.2 mm

5.3 FE simulation of stretch forming

The FE simulations were done to check to check the accuracy of failure prediction in stretch forming of CRDQ steel. The failure predictions based on the developed as well as existing correlations were compared with the experimental results.

The stretch forming simulation was carried out using a 101.6 mm hemispherical diameter punch. The design parameters are given in table 6. The dimension of blank used is 175mm X 175mm and .8mm thickness representing three different modes of deformation namely biaxial stretching, plain strain condition and tension-compression respectively. The punch, die and blank holder were modeled in pre processor and a circular draw bead of 132 mm diameter was defined on the die. The blank was placed at the center of the die.

5.3.1 Design parameters for stretch forming simulations

Table 6   Design parameters

Design parameter	Dimension(mm)
Die diameter	104
Punch Diameter	101.6
Blank holder diameter	255
Die corner radius	10
Draw bead diameter	132
Blank thickness	0.8

All tools were considered to be rigid bodies and they were meshed using 'automesh' option. The blank was considered as a deformable body and it was meshed with quadrilateral shell elements. The default shell element formulation is BELYTSCHKO-TSAY, which is widely implemented in stamping simulation. The minimum size of element used is 0.5 mm for both tool and the blank. The number of thickness integration points is chosen as 7 to get better results at the cost of CPU. Draw bead is defined as line bead and was locked at the die. The 'forming-one-way' type contact interface is used for defining the contact. The arrangement of meshed tools and blank is shown in Fig. 20
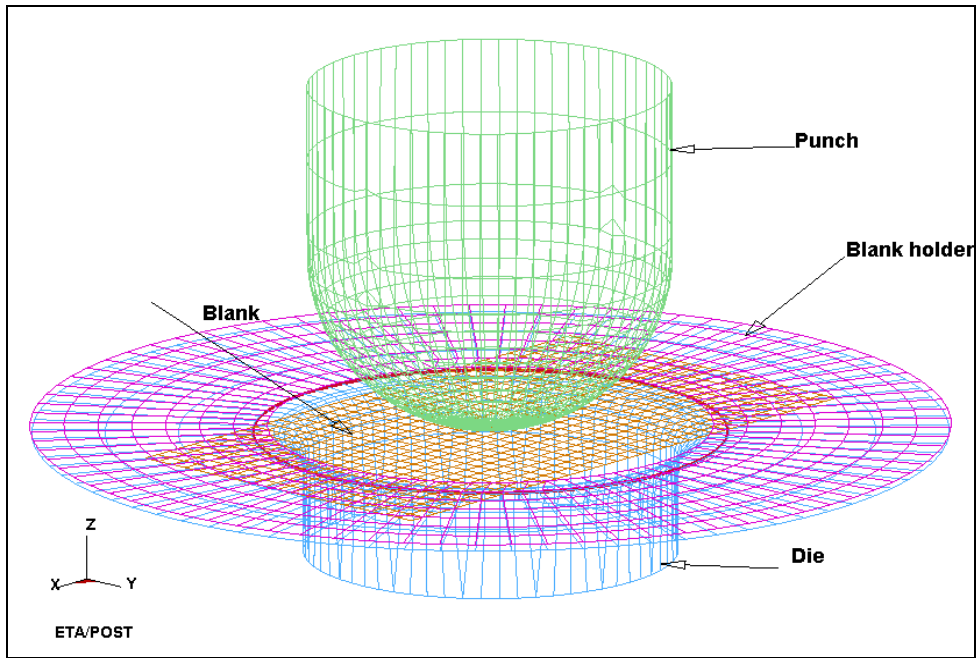
Fig 20 Arrangement of tools and blank in FE simulation
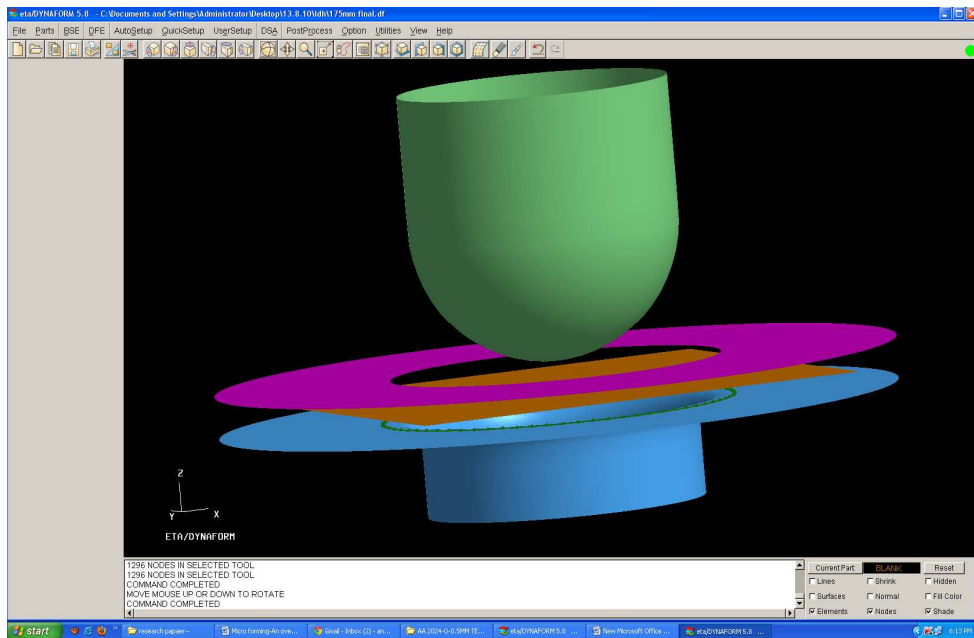
Fig 21. Modelling in Dynaform

5.3.2 Material model

LS DYNA material model no 36 was used to simulate plastic deformation behaviour of blanks during stretch forming. Material model 36 uses Barlat's three parameter plasticity model which incorporates the effect of both normal and planar anisotropy. Material is assumed to be rigid plastic with power law of strain hardening. The true stress-true strain curve was given as input to the material library for performing the simulations. The material properties (as determined from tensile tests) used for the blanks are reported in **Error! Reference source not found.**. The anisotropic yield function is defined as [Barlat, F. and Lian, J., 1989]:

$$f = a|K_1 + K_2|^M + a|K_1 - K_2|^M + c|2K_2|^M = 2(\overline{\sigma})^M$$

where $K_1 = \dfrac{\sigma_{xx} + h\sigma_{yy}}{2}$ and $K_2 = \sqrt{\left(\dfrac{\sigma_{xx} - h\sigma_{yy}}{2}\right)^2 + \rho^2 \sigma_{xy}^2}$

a, c, h and ρ are anisotropic material constants, which can be calculated using anisotropy parameters.

5.3.3 Simulation Results of Biaxial Stretching :

LDH = 39.5mm
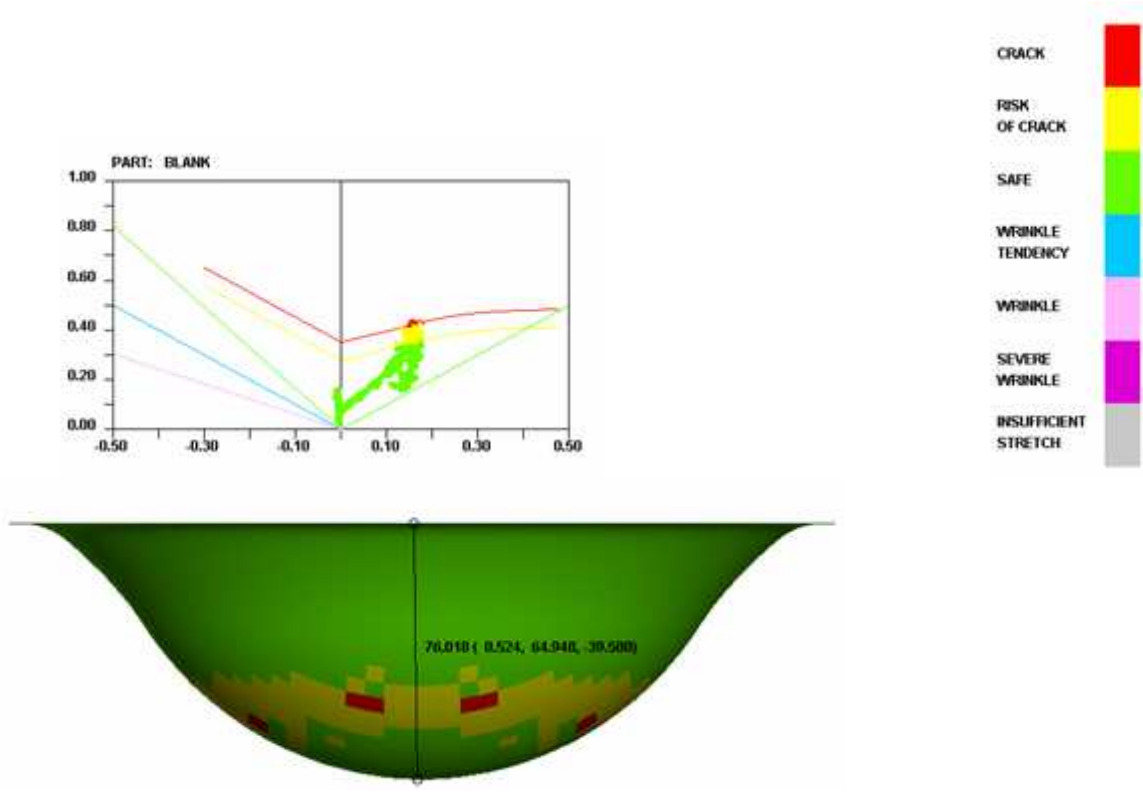
Fig 22. Limiting Dome Height

175mm final

STEP 15   TIME: 0.043637

COMPONENT: Thinning
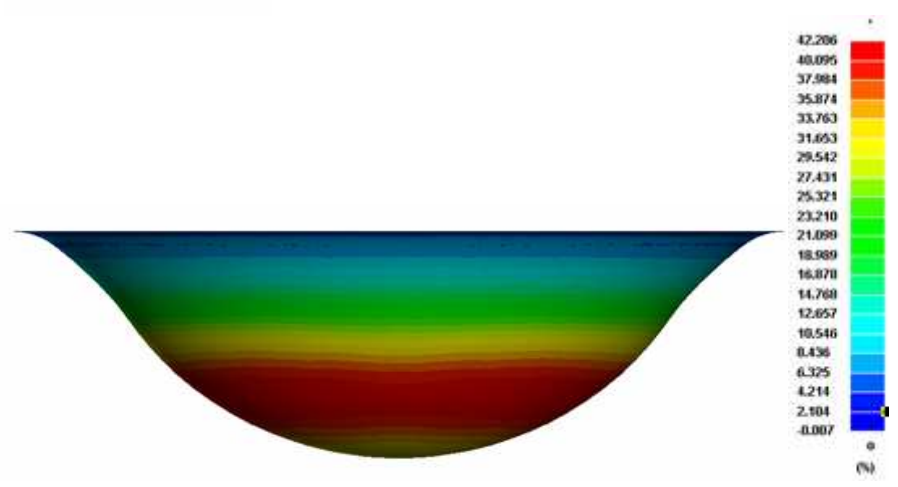
Fig. 23 Thinning Strain in LDH Test

Vonmises stress distribution :
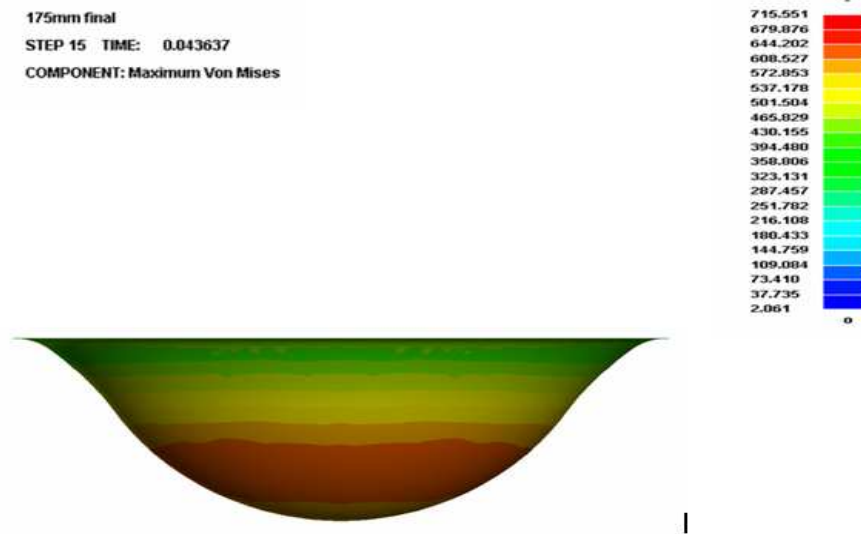
Fig. 24 VonMises stresses

Thickness:
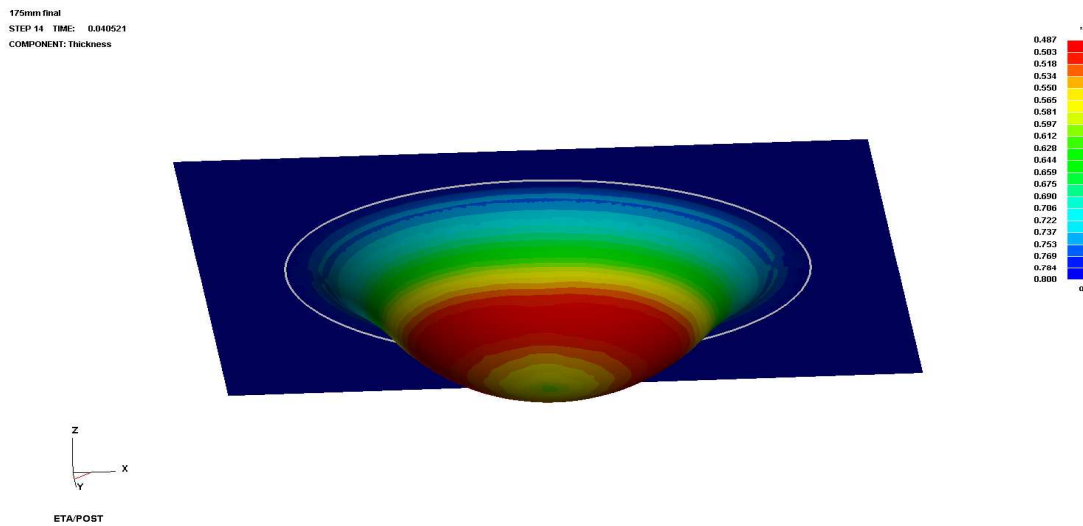
Fig. 25 Thickness Strain

5.4 Experimental results of Fuel tank Exterior of Motor Bike

Fig . 26 Fuel tank exterior without flange

Fig. 27 Fuel tank Exterior with flange

Table 7 Thinning strain for Fuel Tank

Major axis(mm)	Minor axis(mm)	Sheet Thickness(mm)	Major strain (%)	Minor strain (%)	Thinning(mm)
5.84	4.82	0.8	16.8	-3.6	0.710509862
5.9	4.91	0.8	18	-1.8	0.690393179
5.95	4.86	0.8	19	-2.8	0.691634679
6.05	4.84	0.8	21	-3.2	0.683013455
5.87	4.9	0.8	17.4	-2	0.69533776
6.05	4.9	0.8	21	-2	0.674650025
6.17	4.64	0.8	23.4	-7.2	0.698597217
6.25	4.76	0.8	25	-4.8	0.672268908
6.31	4.73	0.8	26.2	-5.4	0.670099811
6.19	4.75	0.8	23.8	-5	0.680214267
6.12	4.83	0.8	22.4	-3.4	0.676599142
5.78	5.09	0.8	15.6	1.8	0.679805032
6.02	4.94	0.8	20.4	-1.2	0.672522092
6.05	4.88	0.8	21	-2.4	0.677414984
5.89	5.02	0.8	17.8	0.4	0.676411502
6.22	4.62	0.8	24.4	-7.6	0.695981403
5.67	4.33	0.8	13.4	-13.4	0.814627451
5.81	4.66	0.8	16.2	-6.8	0.738699741
5.68	4.51	0.8	13.6	-9.8	0.780737641
5.72	4.53	0.8	14.4	-9.4	0.771855076
5.74	4.95	0.8	14.8	-1	0.703903143
6.23	4.24	0.8	24.6	-15.2	0.757139829
5.74	5.18	0.8	14.8	3.6	0.672648756
5.74	4.45	0.8	14.8	-11	0.782993384
5.49	4.65	0.8	9.8	-7	0.783438118
5.77	5.11	0.8	15.4	2.2	0.678317907
5.71	4.69	0.8	14.2	-6.2	0.746828778
5.97	4.91	0.8	19.4	-1.8	0.682298117
6.13	4.81	0.8	22.6	-3.8	0.678304104

% Reduction in sheet thickness experimentally = (0.8-.67) \ 0.8

$$= 16.25 \ \%$$

CHAPTER 6

RESULT & DISCUSSION

Fuel Tank Exterior of Motor Bike has been scanned by using white light scanner and it is imported in HyperMesh for Deep Drawing Analysis. The deep drawing process has been simulated numerically using Hypermesh to predict the range of blank size,blank holding force & Die corner radius for CRDQ steel.The steps involved during the analysis are shown below.

Experimental results used for simulation using hyper-mesh software are shown in table below taken from table no(2) as shown during experimental work.

Table 8 Different Parameters of CRDQ steel used in simulation

Sr.No.	Parameters	Mean value
1.	UTS	244.34 N/mm^2
2.	Yield stress	138.9 N/mm^2
3.	Strain Hardening coefficient	.24
4.	Anisitropy	1.5

Step 1 : Blank Size Optimization
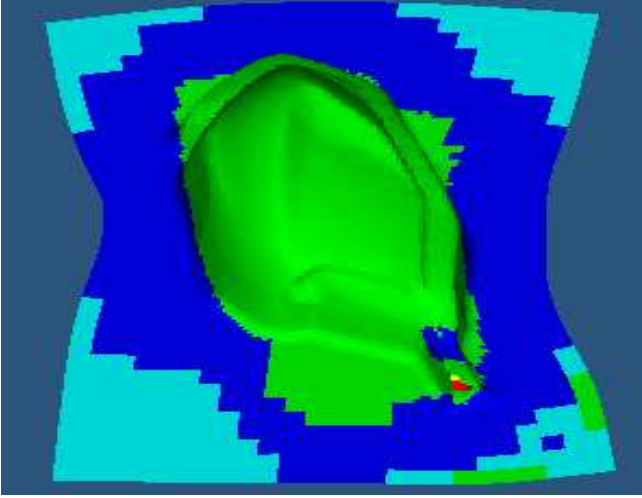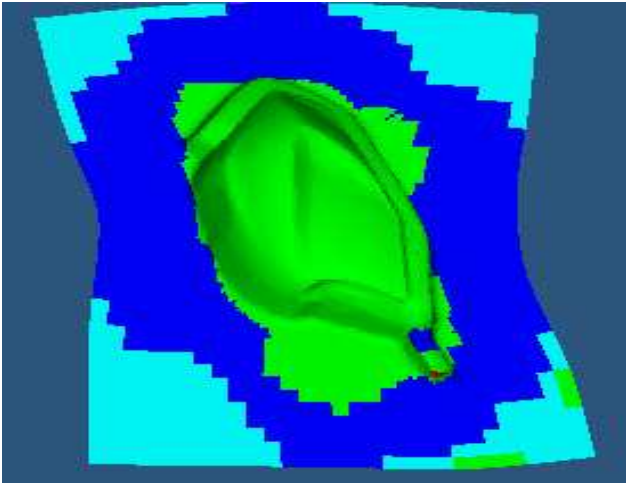
Load : 30 ton as per theoretical calculation (ref)
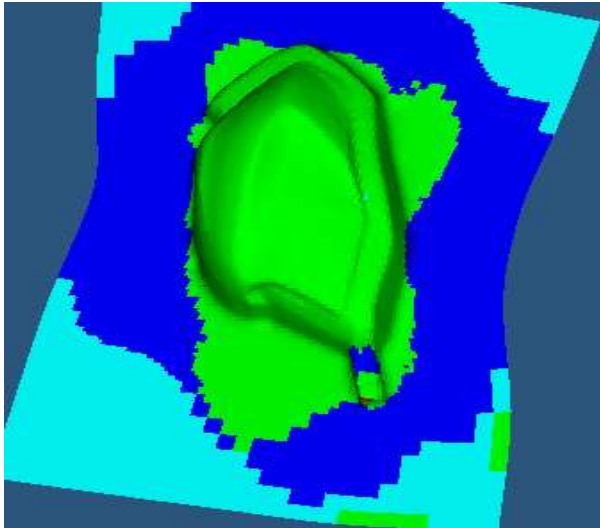
Criterion : Wrinkles on the flange

Remedy : Increasing BHF and provide optimum area under binder.

Various blank size used for experimental analysis

Table 8 Optimization of Blank Size

Blank Size(mm)	Image	Remarks
750 *1050		Excessive Wrinkles on flange and in the component wall
850* 1050		Wrinkles do not penetrate the drawn part as blank width is increased and consequently BH Pr. is reduced marginally.

900 *1100		Wrinkles are still there but not penetrating the component and BH pr. is reduced further.

Conclusion : As the blank area is increased by increasing the size of component the wrinkles are avoided by using an optimum blank holding pressure.

Step 2 : Optimisation of Blank Holding Force : Since blank size is controlling the flange distortion there is another risk of component failure due to wrinkles in wall of component.
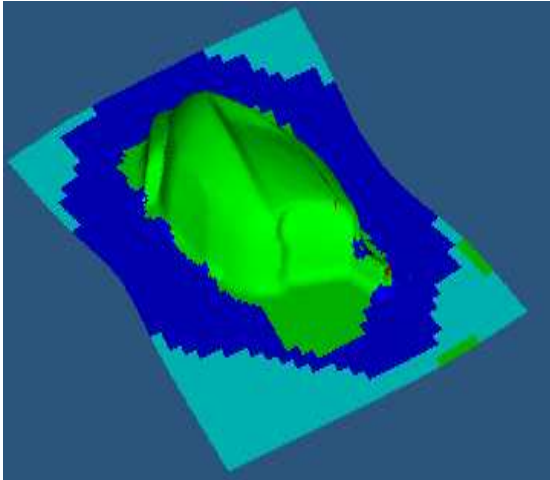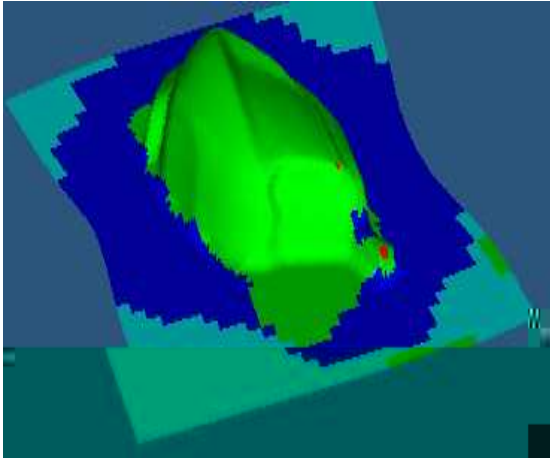
Blank Size : Optimised in step 1 (900mmX1100mm)
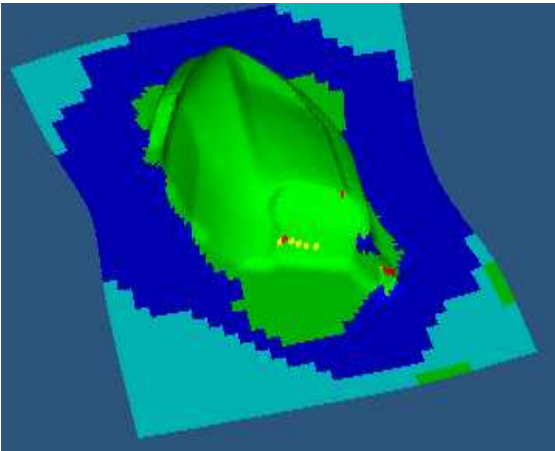
Varying BHF : 30, 25 & 35 tons

Criterion : wrinkles in wall of component

Remedy : Varying Blank holding force

Table 9 Optimization of Blank Holding Force

Optimum Blank Size(mm)	Blank Holding Force (tons)	Image	Remarks
900 *1100	30		Wrinkles are visible on wall of the component.
900 * 1100	25		Amount of wrinkles are increased on the wall of component.

900 *1100	35		There is visible cracks on the wall of the component,results in rejection of the component.

Conclusion : 30 Tons of BHF gives better results in deep draw hence it is taken as the optimum value.As by reducing the BHF there are wrinkles on component wall surface and by increasing the BHF component distorted completely due to induced cracks.
.

Step 3 : Die Corner Radius : After optimizing the blank size & blank holding force, further scope of improvement in geometry of component is possible only by varying Die corner radius..
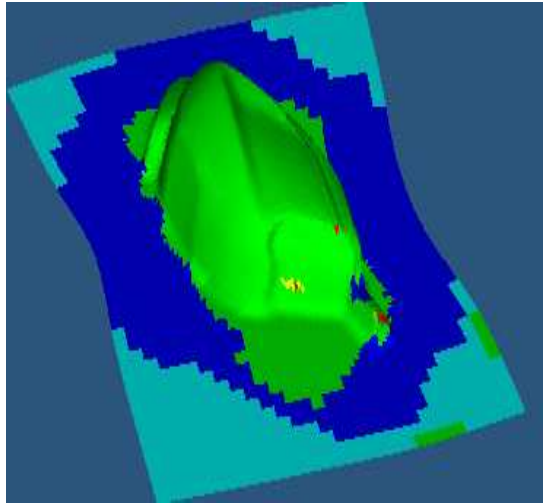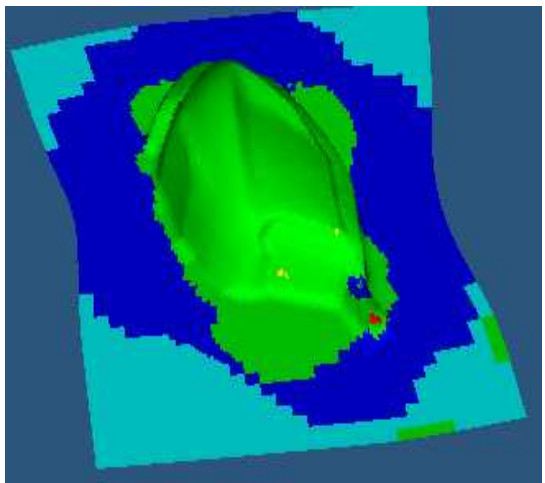
Blank Size : Optimised in step 1(900mm X1100mm)

BHF : Optimised in step 2 (30 ton)

Criterion : Cracks in the component.

Remedy : Increasing Die corner radius

Table 10 Optimization of Die Corner Radius

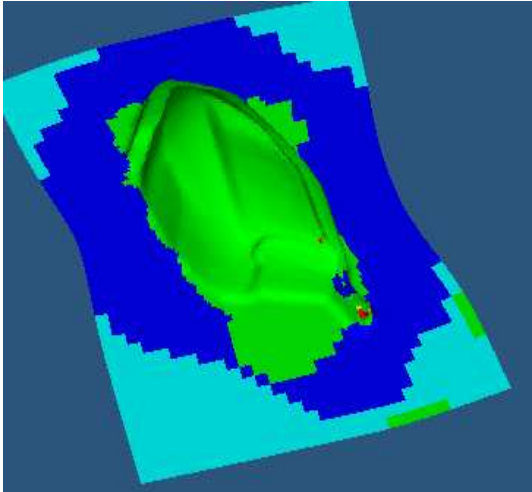| Optimised Blank Size (mm)	Optimised BHF (tons)	Die Corner Radius (mm)	Image	Remarks
900 *1100	30	20		Tearing on the curved surfaces of the component.
900 * 1100	30	22		Marks of thinning observed on the curved surfaces
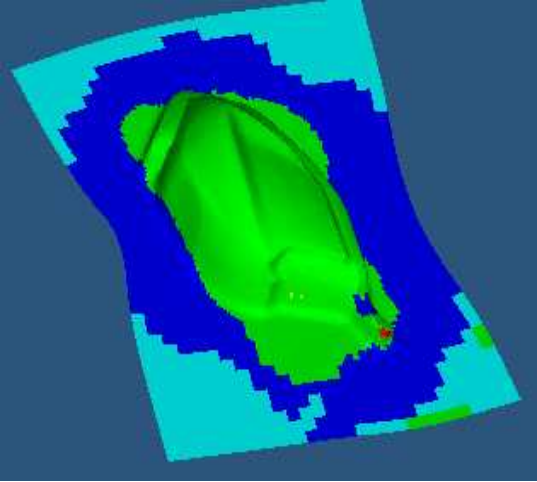
900 *1100	30	25		Light impression of thinning
900 * 1100	30	26		No thinning

Table 9

Conclusion: Die corner radius is regulating the smooth flow of material into the die i.e. higher the die corner radius lesser will be the stresses in the component wall due to less stretching. Too high a die corner radius is resulting in oversizing the component in trimming area, therefore the optimum die corner radius is chosen as 26mm.

Step 4 : Drawbead Analysis : After optimizing the blank size, blank holding force & Die corner radius,further scope of improvement in geometry of component is possible by applying drawbead.

Objective : To reduce the possibilities of cracks in the component by smooth flow of material.
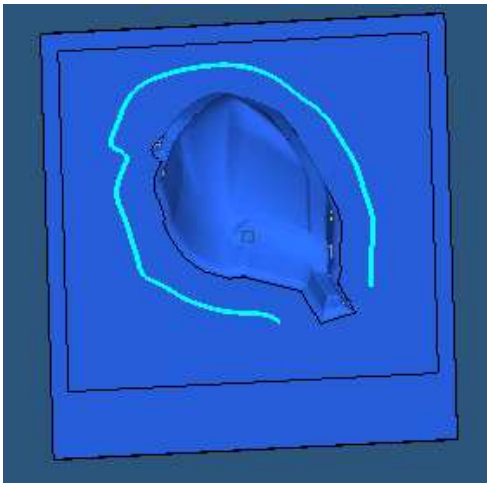
Blank Size : Optimised in step 1 (900mmX1100mm)
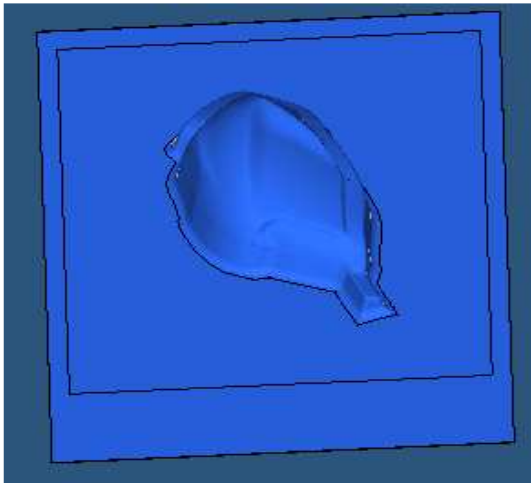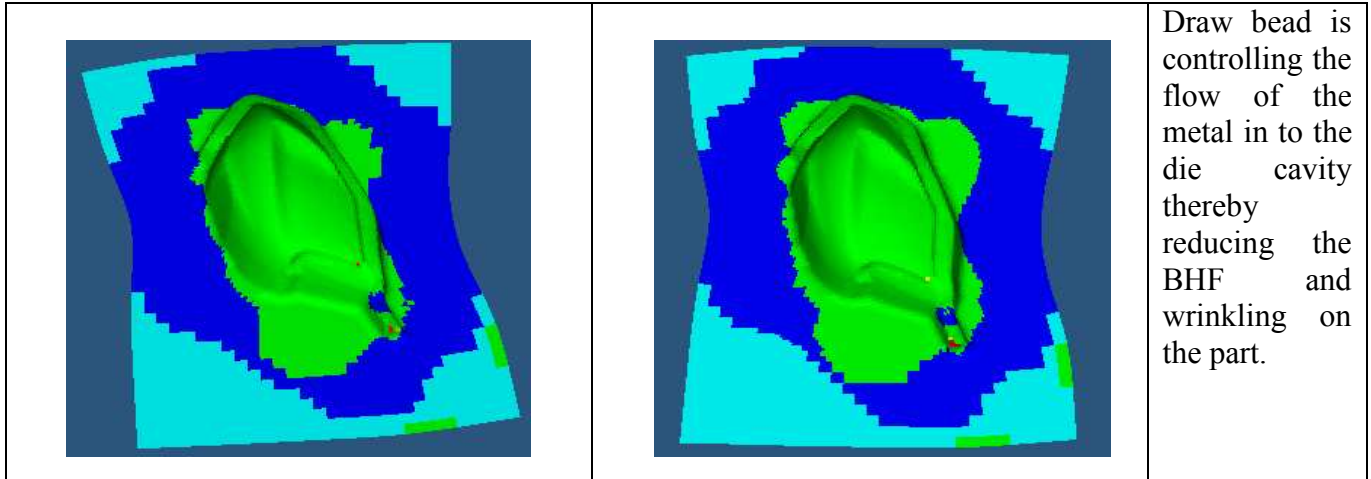
BHF : Optimised in step 1 (30 ton)

Die radius : Optimised in step 1 (26)

Criterion : Impression of thinning

Remedy : Inserting drawbead in binder

Table 11 Drawbead Analysis

Image without Drawbead	Image with Drawbead	Remarks
		Recommended Drawbead size is 16X5 circular .

		Draw bead is controlling the flow of the metal in to the die cavity thereby reducing the BHF and wrinkling on the part.

Step 5 : Thinning Analysis : Since now thinning is not visible on the component through software simulation we analyse the thinning in the component and compare it with the safe(maximum thining) limits of the component calculated experimentally as shown in table no ( ) i.e. .55 mm

% Reduction in sheet thickness experimentally = (0.8-.67) \ 0.8

$$= 16.25\ \%$$

%. Reduction in sheet thickness using simulation software is shown in figure below

So results are compatible with each other.

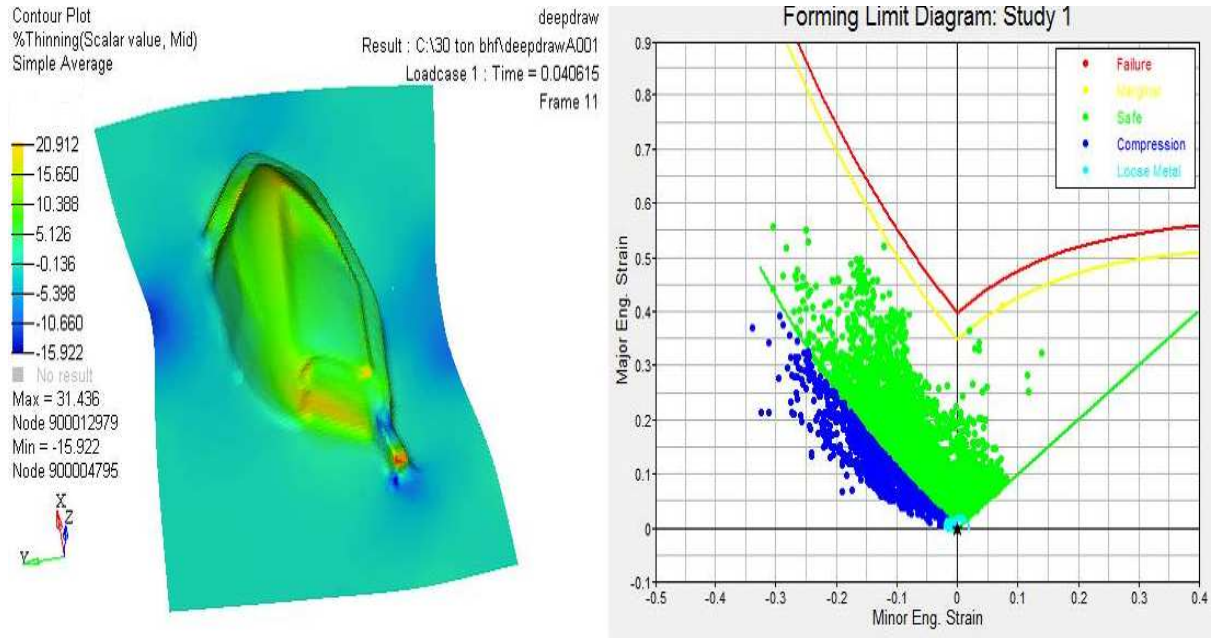Objective : To analyse and compare the thinning with the practical values.
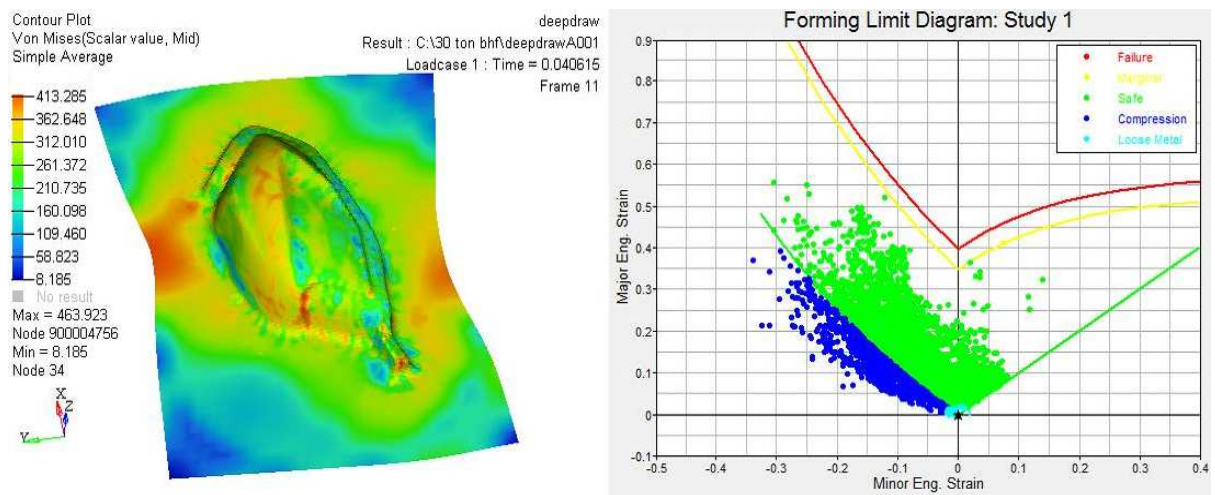
Fig. 28 Thinning results
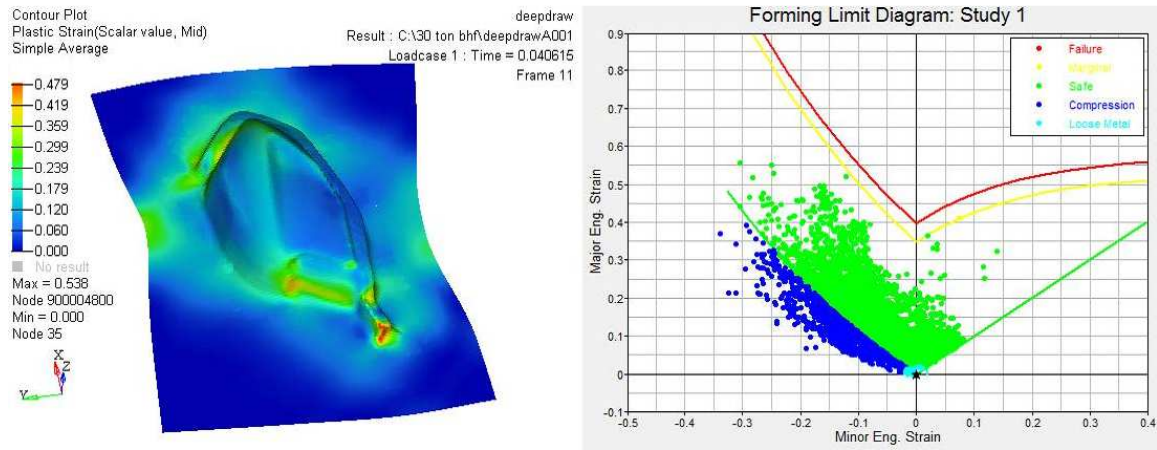

Fig. 29 VonMises Stresses

Fig. 30 Plastic Strain

Step 6: Blank Shape obtained after Re-engineering

This blank shape is obtained through the Radioss one step solution in HyperMesh.Firstly we create a die face and blank and further assign the material and mesh on it, then through tool setup we create required punch and binder .Punch resembles the shape of object to be made, then further we use punch to obtain the original blank shape.
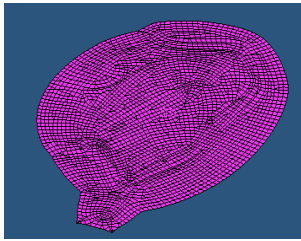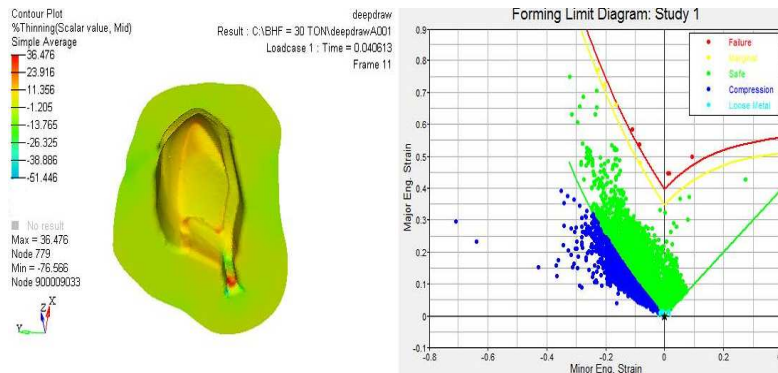

(a)   Original Blank Shape
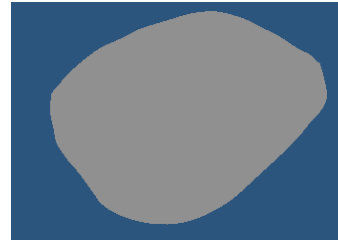
(b) Blank with Addendum
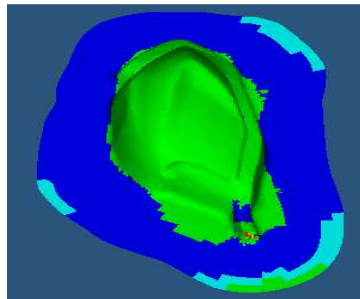
(c) Simulation result

(d) Thinning Strain

Fig. 31 Simulation result of original blank shape

Chapter 7

CONCLUSION

In order to analyse a deep drawing product the finite element simulation is a suitable tool:

1. Material characterization for CRDQ steel is showing close correlation with the simulated results, hence the material model: Barlat three parameter model, used in Dynaform is presenting fair approximation for LDH and strain distribution. Material suitable for complex stampings ought to be characterized by high values of properties such as strain hardening exponent (n) and the plastic anisotropy coefficient (R).

2. Blank Optimization: Results of simulation for blank size optimization is reflecting a modification in the actual blank size used experimentally in the industry, exploring a scope of material saving. Blank shape obtained through Re-engineering is quite complex and it requires additional time and cost. Hence rectangular blanks are more suitable.

3. Optimization of blank holding force is extremely important for avoiding the wrinkling entering into the drawn component. It was observed that in order to avoid wrinkling, the blank holding force should be much higher for producing the deep drawn component. A safe range of BHF has been identified for the deep drawing of the fuel tank exterior.

4. Clearance between the punch and the die should be 7% to 12% more than the sheet thickness as identified. If the clearance is too small the blank may be simply pierced or sheared by the punch.

5. Die Corner radius: Die corner radius should facilitate easy flow of the material into the die cavity but if the die corner radius is too large the component wall may wrinkle, and if it is too small can cause fracture at the corners.

6. Draw bead effect: Drawbeads are often necessary to control the flow of the blank into the die cavity. Draw beads restricts the flow of the sheet by bending and

unbending it during deep drawing, they thereby increase the force required to pull the sheet in to the die cavity. They also help to reduce the required BHF because the beaded sheet has higher stiffness and hence lower tendency to wrinkle. The same has been justified in the final draw results with draw beads.

7.1   Future Scope:

1. The influence of sheet roughness in deep drawing cannot be neglected. The roughness has a significant effect on the punch force: the punch forces increases with increasing roughness height. The relative amount of this influence depends on amount of lubricant, the type of product, the type of sheet metal, and also can vary with the state of the process (punch travel). Differences in punch force reveal themselves in the dimensions of the product after deep drawing, and the sensitivity to fracture as expressed in the fracture limit.

2. Many aspects encountered in deep drawing can be studied successfully by friction tests with simple specimen geometry. The influence of pressure on the position of the Stribeck curve, as encountered in friction tests, can be directly related to phenomena in deep drawing operations.

3. Develop the instrumentation to accurately monitor deformation and growth of wrikling during the process·

REFERENCES

1. D.Ravi Kumar((2002), "Formability analysis of extra-deep drawing steel" Department of Mechanical Engineering, Indian Institute of Technology Delhi, Journal of Materials Processing Technology 130–131 (2002) 31–41

2. Chung S.Y. and Swift.H.W. (1951a), 'Cup drawing from a flat blank, Part 1. Experimental investigation, Proceedings of Institution of Mechanical Engineers, U.K. pp. 199-211

3. Chung S.Y. and Swift H.W. (1951b), 'Cup drawing from a flat blank, Part 2. Analytical investigation, Proceedings of Institution of Mechanical Engineers, U.K. pp. 211-225.

4. Mark Colgan and John Monaghan (2003), 'Deep drawing process: analysis and experiment', Journal of Materials Processing Technology, Vol. 132, pp.35-41

5. Slater R.A.C. (1977), 'Engineering Plasticity', John Wiley and Sons, New York.

6. Marciniak Z., Duncan J.L. and Hu S.L. (2002), 'Mechanics of sheet metal forming", Butterworth Heinemann, London.

7. Hobbs R.M. and Duncan J.L. (1979) Press Forming, Advanced Technology course, Course No.4, American Society for Metals.

8. Johnson W. and Mellor P.B. (1976), 'Engineering Plasticity', John Wiley & Sons, New York.

9. Eary D.F. and Reed E.A. (1958), 'Techniques of Press working sheet Metal', 2nd edition, Prentice Hall, Eaglewood Cliffs NJ.

10. Swift H.W. (1939-40), 'Drawing tests for sheet metal', Proceedings of Institution of Automobile Engineering, Vo1.34, p.361.

11. Whiteley R.L. (1960), 'The importance of directionality in drawing quality sheet steel', Transactions of American Society of Mechanical Engineers, Vo1.52, p-.154.

12. Wilson F.W., Hartley P.D and Gump C.B. (1965), 'Die Design Handbook', Society of Manufacturing Engineers, McGraw Hill, New York.

13. Mellor P.B. and EI-Sebaie M.G. (1972), 'Plastic Instability conditions in the deep-drawing of a circular blank of sheet metal', International Journal of Mechanical Sciences, Vol. 14, pp. 535-540.

14. Yoshida K. and Miyauchi K. (1978), 'Experimental studies of Material Behaviour as

related to sheet metal forming", Mechanics of Sheet Metal forming, General Motors Research Laboratories, Plenum Press, pp.19-52.

15.   Newnham lA. (1970), 'Metal deformation processes friction and lubrication, Marcel Dekker, New York.

a.   Avitzur B. (1982), 'Upper bound analysis of deep drawing', Proceedings of North American Metal working Research Conference (NAMRC), Hamilton.

b.   Meuleman D.J. (1980), 'Effects of mechanical properties on the deep drawability of sheet metals', PhD dissertation, University of Michigan.

c.   Lange K. (1985), 'Handbook of Metal Forming', McGraw Hill, New York.

d.   Keijiro Suzuki (1987), 'The relationship between the deep drawability and the r-values of sheet metals', Journal of Mechanical Working Technology, Vol. 15, pp.131-142.

e.   Min Wan, Yu-Ying Yang and Shuo-Ben Li (2001) 'Determination of fracture criteria during the deep drawing of conical cups', Journal of Materials Processing Technology, Vol. 114, ppJ09-113.

f.   Jan Havranek (1977), 'The effect of mechanical properties of sheet steels on the wrinkling behaviour- during deep drawing of conical shells', Journal of Mechanical Working Technology, Vo1.1, pp.115-129.

g.   Majlessi S.A. and Lee D. (1993a), 'Deep drawing of square-shaped sheet metal parts, Part-I, Finite element analysis', Transactions of ASME, Vol.ll5, pp. 102-109.

h.   Majlessi S.A. and Lee D. (1993b), 'Deep drawing of square-shaped sheet metal parts, Part-2, Experimental study', Transactions of ASME, Vol. 115, pp. 110-117.

i.   Mamalis A.G., Manolakos D.E. and Baldoukas A.K. (1997a), 'Simulation of sheet metal forming using explicit finite element techniques: Effect of material and forming characteristics Part 1. Deep drawing of cylindrical cups', Journal of Materials Processing Technology, Vol. 72, pp.48-60.

j.   Mamalis A.G., Manolakos D.E. and Baldoukas A.K. (1997b), 'Simulation of sheet metal forming using explicit finite element techniques: Effect of material and forming characteristics Part 2. Deep drawing of square cups', Journal of Materials Processing Technology, Vol.72, pp.ll0-116.

k.   Hiroshi Koyama, Ken-ichi Manabe and Shoichiro Yoshihara (2003), 'A database oriented process control design algorithm for improving deep drawing performance', Journal of Materials Processing Technology, Vol.138, pp. 343-348.

l. Yang D.Y., Lung D.W., Song I.S., Yoo D.J. and Lee J.H. (1995), 'Comparative investigation into implicit, explicit, and iterative implicit/explicit schemes for the simulation of sheet-metal forming processes', Journal of Materials Processing Technology, Vo1.50, pp.39-53.

m. Leonid Shulkin, Steven W. Jansen, Mustafa A. Ahmetoglu, Gary L. Kinzel and Taylan Altan (1996), 'Elastic deflections of the blank holder in deep drawing 'of sheet metal', Journal of Materials Processing Technology, Vo1.59, pp.34-40.

n. Plevy T.A.H. (1980), 'The role of friction in metal working with particular reference to energy saving in deep drawing', Journal of Wear, Vo1.58, pp. 359-380.

o. Tsung-Sheng Yang (1999), 'Full film lubrication of deep drawing', Journal of Tribology International, Vo1.32, pp.89-96

p. Bilgin Kaftanoglu (1973), 'Determination of coefficient of friction under conditions of deep drawing and stretch forming', Journal of Wear, Vol.25, pp. 177-188.

q. Jung D.W., Song 1.S. and Yang D.Y (1995) 'An improved method for the application of blank-holding force considering the sheet thickness in the deep-drawing simulation of planar anisotropic sheet', Journal of Materials Processing Technology, Vo1.52, pp. 472 -488

r. Hematian 1. and Wild P.M. (2001), 'The effects of tooling imperfections on the initiation of wrinkling in the finite element modeling of a deep drawing process', Transactions of ASME, Vol. 123 , pp. 442-446.

s. Sosnowski W., Onate E. and Agelet de Saracibar C. (1992), 'Comparative study on sheet metal fonning processes by numerical modeling and experiment', Journal of Materials Processing Technology, Vo1.34, pp 109-116.

t. Claudio Garcia, Diego Celentano, Fernando Flores and Jean-Philippe Ponthot (2005a), 'Numerical modelling and experimental validation of steel deep drawing processes Part I: Applications', Journal of Materials Processing Technology, Vol. 172, pp. 451-460.

u. Claudio Garcia, Diego Celentano, Fernando Flores, Jean-Philippe Ponthot and Omar Oliva (2005b), 'Numerical modelling and experimental validation of steel deep drawing processes Part II: Applications', Journal of Materials Processing Technology, Vol. 172, pp.461-471.

v. Zaky A.M., Nassr A.B. and EI-Sebaie M.G. (1998), 'Optimum blank shape of

cylindrical cups in deep drawing of anisotropic sheet metals', Journal of Materials Processing Technology, VoL76, pp.203-211.

37   David Roylance (2001) 'Department of Materials Science and Engineering'Massachusetts Massachusetts Institute of Technology, Cambridge, MA 02139

38   G.E. Dieter, Mechanical Metallurgy, McGraw-Hill, London, 1988,pp. 295-301.

39   W.F. Hosford, R.M. Caddell, Metal Forming-Mechanics and Metallurgy, Prentice Hall, USA, 1993, 270-308.

40   R. Cada(1996), 'Comparison of formability of steel strips, which are used for deep drawing of stampings' Journal of Materials Processing Technology 60 ,pp. 283 -290